Journal of Materials Chemistry A

Accepted Manuscript

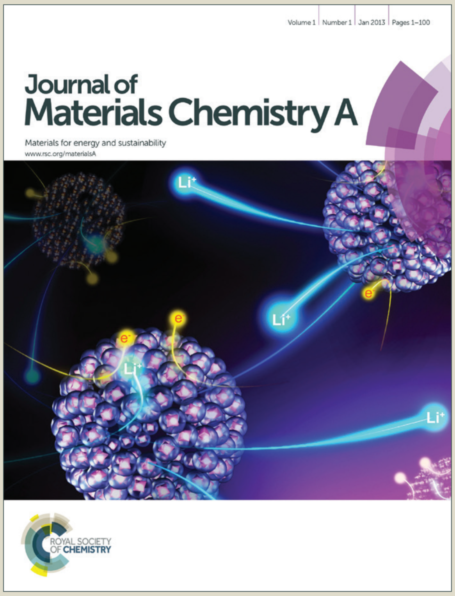

ROYAL SOCIETY OF CHEMISTRY

www.rsc.org/materialsA

Editor of Journal of Materials Chemistry A

January 21, 2015

Dear Prof. Skinner,

We submit the new version of the manuscript, revised according to the reviewers' recommendations along with the detailed reply to their comments. We are grateful to the reviewers for careful revision of our paper. We have addressed their useful comments and replied all of them. We decided to include some of our answers to the manuscript in order to strengthen it. As a consequence, the manuscript has been modified accordingly. For those comments we did not agree with, we provided detailed explanations supported with the literature references where it is suitable.

Yours sincerely,

On behalf of co-authors

Mr. Vladimir Sereda

Replies to the referees

Referee: 1
Comments to the Author
The considered paper shows interesting results and detailed discussion of selected physiochemical properties of LaNi0.6Fe0.4O3-d perovskite, and brings significant improvement, comparing to the initial submission.
Nevertheless, before publication, I encourage the Authors to answer the following questions, and update the manuscript correspondingly:

1) It was stated that charge carriers in LaNi0.6Fe0.4O3-d can be considered as localized. However, the reported conductivities exceed 100 Scm-1. This seems to be a contradiction.

We cannot agree with Referee 1 that conductivity value of 100 S/cm is in a contradiction with the localized nature of the carriers. Actually, even conductivity of $LaCoO_3$ (more than 1000 S/cm, which is an order of magnitude higher than that of $LaNi_{0.6}Fe_{0.4}O_{3-\delta}$) is quite consistent with the small polaron conduction mechanism (S.R. Sehlin, H.U. Anderson and D.M. Sparlin[1]). Indeed, the prefactor in the expression for the temperature dependence of adiabatic small polaron conductivity[2] $\sigma_i \propto \frac{1}{T}\exp(-\frac{E_a}{kT})$ gives rise to the possibility of a conductivity that decreases with increasing temperature in the limit that T is high and E_a is low. Typical mobilities for adiabatic small polaron hopping are of the order 0.1 $cm^2/(V*sec)$ (please compare to mobility values found by us and shown in Fig. 12 of the manuscript). Then the expression for conductivity $\sigma_i = e|z_i|n_i U_i$, where z=1, *e* is electron charge, *U* is mobility and *n* is carriers concentration, yields 1000 S/cm at $n \sim 10^{23}$ carriers/cm^3. It means simply that a significant molar fraction of the conduction sites must contain charge carriers.

We would also like to emphasize in addition that in the recent comprehensive review on materials development for IT SOFCs well-known authors from Imperial College London[3] conclude that despite topic on the transport mechanism for undoped and doped high conducting perovskites such as $LaCoO_3$ still remains controversial, better explanation of available experimental data on the oxygen nonstoichiometry[4,5,6] and Seebeck coefficient[1,7] as well as chemical expansion[8] can be given on the basis of the existence of small polarons on the cobalt sites. The same was also concluded for the lanthanum ferrite doped with Ni, $LaFe_{0.7}Ni_{0.3}O_{3-\delta}$. [9] It was found that its defect structure "can be described in terms of randomly distributed point defects within a small polaron concept of electronic defect state."[9] The oxygen nonstoichiometry of 0.5% A-site cation deficient ferrite $La_{0.6}Sr_{0.4}Co_{0.2}Fe_{0.8}O_{3-\delta}$ was studied in the temperature range of 600–900°C and modeled using a metallic model and three semiconductor models assuming itinerant electrons and holes or electrons localized on B-site, cations, with holes

---

[1] S.R. Sehlin, H.U. Anderson, D.M. Sparlin, Phys. Rev. B., V. 52 (1995) 11681-11689
[2] D. Emin, T. Holstein, Am. Phys. (N.Y.) 53, 439 (1969)
[3] S.J. Skinner et al., J. Mater. Sci., 2012, v. 47, 3925-3948
[4] A.N. Petrov et al., Solid State Ionics, 1995, v. 80, 189-199
[5] V.L. Kozhevnikov et al., Journal of Solid State Chemistry, 2003, v. 172, 296-304
[6] A.Yu. Zuev et al., J. Mater. Sci., 2007, v. 42, 1901
[7] A.N. Petrov et al., J. Mater. Sci., 2007, v. 42, 1909
[8] A.Yu. Zuev et al., Solid State Ionics, 2008, v. 179, 1876-1879
[9] E.A. Kiselev, V.A. Cherepanov, Solid State Ionics, 2011, v. 191, 32-39

localized on either B-site cations or oxygen anions. The model consisting of holes localized on B-site cations was found to fit the obtained data best[10].

Finally, the results of very interesting computational works of D. Marrocchelli , S.R. Bishop et al.[11,12] should be mentioned. These authors showed strong correlation between the degree of electronic defects localization and chemical expansion or, in other words, only large degree of the electronic defects localization in the compound may cause chemical expansion of its lattice. It seems to be the case of $LaNi_{0.6}Fe_{0.4}O_{3-\delta}$.

Taking into account all aforementioned as well as the results of our study itself, we believe the holes and electrons in $LaNi_{0.6}Fe_{0.4}O_3$ to be the localized charge carriers and, therefore, that small polaron hopping is the reliable mechanism of its overall conductivity.

2) Charge disproportionation reaction (Eq. 4) is of course correct, but as it is known that in various Fe-containing perovskites a disproportionation of: 2Fe4+ to Fe5+ and Fe3+ can take place, at least, this should be mentioned as a case, which is not considered in the presented model.

We agree with Referee 1 that the disproportionation reaction $2Fe^{4+}=Fe^{5+}+Fe^{3+}$ was found to occur in some perovskite oxides. Takano et al.[13] and Takeda et al.[14] were the first who described this reaction for $CaFeO_3$. However, available experimental data seem to indicate in favor of such disproportionation only at temperatures lower than 300 K[13,14,15,16,17,18]. This temperature range is obviously out of the scope of our work. We can cite a large number of publications[19,20,21,22,23,24] supporting the reaction $2Fe^{3+}=Fe^{2+}+Fe^{4+}$ in Fe-contained perovskites at elevated temperatures, i.e. significantly higher than room temperature (the case of the present study). Nevertheless we found that the referee suggestion makes sense and decided to modify the manuscript accordingly. Necessary elucidation has been added to the manuscript *(Section 3.2, after the Eq. 3)*.

3) I still have serious doubts about presence of LS Fe3+. However, the Authors presented their opinion about it, and provided evidence pointing at such the explanation (including LS-HS transition). But again, why no discussion was provided about possibility of such the transition for Ni3+ cations? The magnitude of changes of ionic radii for Fe3+ and Ni3+ cations (in LS-HS transition) are actually comparable.

As we pointed out in the manuscript, there are some evidences in favor of the Fe^{3+} spin-state transition with temperature in the literature whereas data on the HS-LS transition for the Ni^{3+}

---

[10] S. R. Bishop, K. L. Duncan, and E. D. Wachsman Journal of The Electrochemical Society, 156 (10) B1242-B1248 (2009)

[11] D. Marrocchelli , S.R. Bishop , H.L. Tuller , B. Yildiz, Adv. Funct. Mater. **2012**, 22, 1958–1965

[12] D. Marrocchelli, S.R. Bishop, H.L. Tuller, G.W. Watson, B. Yildiz, Phys. Chem. Chem. Phys., 2012, **14**, 12070–12074

[13] Takano M., Nakanishi N., Takeda Y., Naka S. and Takada T., Mat. Res. Bull. 2 (1977) 923.

[14] Takeda Y., Naka S., Takano M. Shinjo T., Takada T., and Shimada M., Mat. Res. Bull. 2 (1978) 61.

[15] P.D. Battle, T.C. Gibb, S. Nixon, J. Sol. St. Chem., 77 (1988) 124-131

[16] K. Świerczek et al. / Solid State Ionics, 2006, v. 177, 1811-1817

[17] J. Marzec / Journal of Power Sources, 2007, v. 173, 671-674

[18] M. Gateshki et al. / Journal of Solid State Chemistry, 2008, v. 181, 1833-1839

[19] M. Idrees et al. / J. Phys. D: Appl. Phys., 2011, v. 44, 455303

[20] Jones and Islam, Journal of Physical Chemistry C, 2008, v. 112, 4455-4462

[21] T. Hashimoto et al., Hyperfine Interact, 2012, v. 206, 47-50

[22] M. Idrees et al. / Current Applied Physics, 2013, v. 13, 448-452

[23] A.E. Goetha et al., Hyperfine Interactions, 1994, v. 90, 371-375

[24] E.A. Kiselev, V.A. Cherepanov, Solid State Ionics, 2011, v. 191, 32-39

ions are absent. In fact, the difference in crystal radii for HS and LS Fe^{3+} is (0.785-0.69)=0.095 Å which is more than two times greater than that for Ni^{3+} - (0.74-0.7)=0.04 Å.[25] Therefore, the ionic radii for high- and low-spin Ni^{3+} are close to each other and it seems to be almost impossible to detect the spin state transition for Ni^{3+}, even if one exists, by means of the dilatometric measurements. Indeed, as seen in Fig. 6 of the manuscript the chemical expansion measured at 950 °C exceeds the one measured at 900 °C at the same value of the oxygen nonstoichiometry. This behavior can be explained neither by an influence of the temperature dependence of the equilibrium constant, K_4, of charge disproportionation reaction Eq. 4, since the one is negative as follows from Table 2 and, therefore, would lead contrariwise, nor by Ni^{3+} spin-state transition due to small difference in radii of HS and LS states of this cation.

So we do not speak that we have already proved the lack of Ni^{3+} spin-state transition, because we simply understand that we cannot confirm it by means of conventional dilatometry and that this one does not influence the chemical expansion of the $LaNi_{0.6}Fe_{0.4}O_{3-\delta}$ lattice.

Taking into account all mentioned above we agree with the Referee that we should point out in the manuscript the reasons for excluding the Ni^{3+} spin-state transition from the chemical expansion model. As a result, the manuscript has been modified accordingly *(a paragraph has been added to Section 3.3, page 6)*.

Referee: 2
Comments to the Author
The authors present experimental measurements of oxygen non-stoichiometry, thermal/chemical expansion, electrical conductivity, and Seebeck effect on a La(Ni,Fe)O3 compound. Though there have been several studies in the past on the same composition, the authors state there are significant discrepancies in the literature. The authors also interpret their data using point defect modeling. The experimental results appear adequate (except for some irreversibility in expansion discussed below), however, the interpretation relies on a variety of fit variables of which their sensitivity in the model is unclear and assumptions which are not adequately justified in the manuscript.

Isothermal expansion data shown in figure 1 is not reversible (i.e. there is a net shrinkage of the sample after returning to pO2's approximately the same as those in the beginning of the measurement), how was this accounted for when making plots of expansion vs. pO2 and delta (figs. 5 and 6)? This explanation needs to be stated in the manuscript text.

We agree with Referee 2. Indeed, Fig. 1 is incorrect. We have to apologize for that. However, the apparent "net shrinkage" is actually observed because the different curves measured at different temperatures were depicted in one plot as though they belong to the same temperature. *We have modified Fig. 1* in the manuscript accordingly. Now it (i) really represents the chemical expansion data measured at one temperature, 950°C, and (ii) contains a relative expansion (left Y-axis) so one could easily compare the data on chemical expansion given in Figs. 1 and 5.

The authors should report the error on their enthalpy values. In particular, what is sensitivity of the enthalpy for the charge disproportionation reaction to fitting, with all

---

[25] R. D. Shannon, Acta Crystallographica Section A, 1976, 32, 751–767.

other variables fixed, can it vary a lot without a significant change in non-stoichiometry? This could dramatically change the values extracted for mobility, etc., in the electrical conductivity section.

We completely agree with Referee 2 that values of the enthalpies can significantly influence ones of the mobilities. However, the error for the enthalpy values was relatively low and did not exceed 10%. During the fitting procedure we used several sets of initial values of the fitting parameters and in all cases fitting procedure was stable and converged to the same values of fitting parameters within the error range mentioned above. We agree with Referee 2 that it should be mentioned in the manuscript, which, therefore, has been modified accordingly *(last paragraph of the Section 3.2).*

It should be also noted that the data on the oxygen nonstoichiometry used for fitting were completely reversible and, therefore, they cannot serve as a systematic error of the enthalpy calculation.

In equation 5, why not start their "K" nomenclature with the subscript 1 and not, as they do now, 3?

That is simply because of the equation numbering system used in our manuscript! Since K_3 is the equilibrium constant for the defects reaction represented by Eq. 3, it is more suitable and convenient to use the constants subscripts corresponding to the number of appropriate defects equilibrium.

Equation 7 has almost no physical basis, how can one predict that change in lattice parameter of a material by simply adding up the size of all the constituent elements with a complete disregard for crystal structure and its bonding arrangements?

We cannot agree with Referee 2. The Eq. 7 of the manuscript has been proposed for isotropic (i.e. cubic or pseudo-cubic) closely packed solid oxides. Let us illustrate the "physical basis" for the model used for chemical expansion calculation. For the sake of simplicity let us consider a closely packed 2D-lattice consisting of two types of ions with different radii, for example, 0.69 Å and 1.26 Å (see Fig. 1 *a* below). The cell parameter is obviously equal to 3.9 Å or double distance between the adjacent ions (1.95 Å).

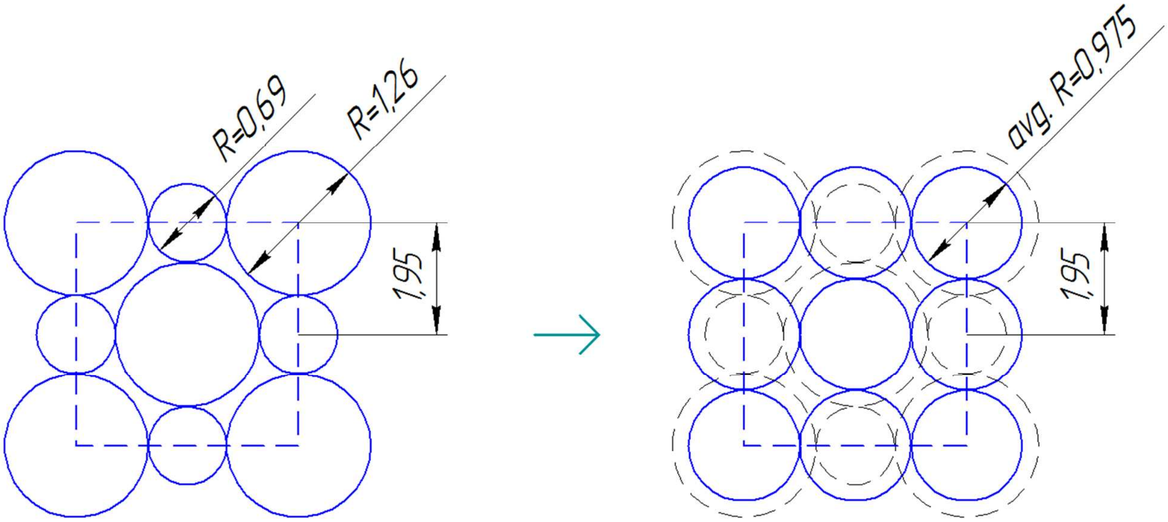

a *b*

Fig. 1. “Equivalent” representations of closely packed 2D-lattice.

From the dimensional point of view the equivalent lattice can be reproduced if real ions are substituted by ions with averaged radii as shown in Fig. 1 *b*. The cell parameter will be obviously the same. The radius of the averaged ion is equal to weighted sum of real ionic radii: $R_{avg} = \frac{c_1R_1 + c_2R_2}{c_1 + c_2} = \frac{\sum c_iR_i}{\sum c_i}$, where c_1, c_2 are numbers (or concentrations in common case) of real ions in 2D-lattice and R_1, R_2 – are their real radii. Any change of the real ion radii will, therefore, lead to corresponding proportional change of an averaged ion radius. The cell parameter is just 4 times R_{avg}. Therefore, normalized change of the lattice parameter is equal to $\frac{\Delta a}{a_0} = \frac{R_{avg} - R^0_{avg}}{R^0_{avg}} = \frac{\sum c_iR_i - \sum c^0_iR^0_i}{\sum c^0_iR^0_i}$, where c_i and R_i – are concentrations and radii of ions, respectively, in the material under current conditions, and c_i^0 and R_i^0 – are concentrations and radii of ions in the material under reference conditions. This is exactly the model Eq. 7 in the manuscript.

We cannot agree also that we do not take into account the oxide crystal structure and bonding arrangement at all. As for the bonding arrangements, we employ in the calculations crystal ionic radii of the ions with coordination numbers well established for the crystal structure of the compound modeled. And, speaking about the crystal structure, we mentioned in the manuscript that the expansion of the lattice is treated within the framework of model approach as isotropic one. This is valid only for cubic or pseudo-cubic structure as one of LNF64. An interesting comparison between the isotropic and anisotropic expansion of the perovskite oxides has been made in our resent paper.[26] This comparison clearly shows the applicability limits of the proposed chemical expansion model.

We would like to emphasize in addition that, a physical basis of the ionic radius is the subject for serious debates since it is known that ions are something more than just rigid spheres, strictly speaking, nevertheless, this approach remains as an useful tool in crystallography, physical chemistry and material science. Regarding our model approach – nobody says that the oxides, in fact, consist of the closely packed lattice of the spherical ions with the equal “mean radius” for each of them. Nevertheless, such simple approach not only allows to calculate correctly the chemical expansion of variety of oxide compounds[27,28,29,30] on the basis of their defect structure model, but to enable understanding of the origin of the chemical expansion phenomenon, which consists more likely in the change of the ionic radii due to reducible ion oxidation/reduction during the oxygen exchange between an oxide lattice and surrounding gas atmosphere.

If the authors are correct, and there is a spin state change with temperature, then equation 10 will not reflect that spin state change unless the thermal expansion coefficient is allowed to change for this material (due to the spin state change). There is almost no change in

---

[26] A. Yu. Zuev, V. V. Sereda, and D. S. Tsvetkov // J. Electrochem. Soc. 2014 161(11): F3032-F3038;

[27] A. Yu. Zuev, A. I. Vylkov, A. N. Petrov and D. S. Tsvetkov, Solid State Ionics, 2008, 179, 1876 – 1879.

[28] A. Yu. Zuev and D. S. Tsvetkov, Solid State Ionics, 2010, 181, 557 – 563.

[29] A. Yu. Zuev, V. V. Sereda and D. S. Tsvetkov, Journal of The Electrochemical Society, 2012, 159, F594–F599.

[30] M.-B. Choi et al. / Acta Materialia 65 (2014) 373–382

oxygen content as the sample is heated in air (see fig. 2), meaning that there will be nearly zero "chemical expansion" in equation 10.

We agree with Referee 2. Indeed, in the absence of phase transition and at constant oxygen content spin state transition should lead to some curvature of thermal expansion. Moreover, in general, pure thermal expansion itself, strictly speaking, is not a linear function of temperature. This overall nonlinearity can be seen in Fig. 8 of the manuscript in the narrow temperature range 800-950°C where such spin transition take place according to our results. However, the largest deviation from the linear behavior can be seen in Fig. 8 at temperatures higher than 1000 °C when the oxide loses significantly lattice oxygen. Therefore, in principle we have, at least, three sources of nonlinearity of the sample length change with temperature: (i) nonlinear behavior of thermal expansion itself, (ii) spin state transition and (iii) chemical expansion. Eq. 10, of course, reflects only one of them i.e. chemical expansion, because thermal expansion coefficient is constant in this case. However, it does not mean that the Eq. 10 is not enough flexible to reproduce expansion curve at all. As seen in the Table 3 of the manuscript the goodness of fit criteria R^2 is very close to 1. Nevertheless, close inspection of the inset in Fig. 8 shows that the fitted curve lies a bit lower than experimental points at around 1100 K and one is not enough curved at around 1350 K. The chemical expansion coefficient fitted, as a result, can be used only for rough estimation of the chemical expansion because it does not reflect completely the sample chemical expansion behavior at given temperature. As seen in Table 3 of the manuscript fitted chemical expansion coefficient is larger than that measured experimentally at 850-900 °C and, on the contrary, smaller than experimental one at 950-1000 °C. All mentioned above means that Eq. 10 is illustrative rather than precise. We mentioned this fact in the manuscript.

Finally, the only reason why we included the Eq. 10 in the manuscript is to convince readership to be careful with employment of this equation since one is frequently used for extraction of the chemical expansion constituent from overall thermal expansion of SOFC materials.

Since there is almost no change in oxygen content on heating in air, the authors need to mention in the manuscript the possibility of a phase transition, or change in crystal symmetry (i.e. tilting), from 800 to 1100 that gives the gradual increase in thermal expansion as opposed to the change in spin state of the Fe cations (though as mentioned above, is not properly accounted for in the present model). Given the large ambiguity in the literature the authors mention on phase stability of this material, it wouldn't be a surprise to find a high temperature phase transition here.

We cannot agree with Referee 2. First of all, we cannot share referee's confidence in "large ambiguity" in the literature on the phase stability of LNF64 since, as it was mentioned in the Introduction section of the manuscript, two papers, which deal directly with the LNF64 stability, are in agreement with each other,[31,32] that this compound is stable up to 1200°C in air. This result is obviously in contradiction with another work[33], where decomposition is proposed for LNF64 at the temperatures above 800°C in air but this proposal is pure hypothesis, which is not proved at all. Therefore, it makes sense to regard LNF64 as stable phase up to 1200°C in air. Moreover, by means of the coulometric titration we have detected obviously (see Fig. 2 of the manuscript)

---

[31] T. Ohzeki, T. Hashimoto, K. Shozugawa and M. Matsuo, Solid State Ionics, 2010, 181, 1771 – 1782.

[32] E. A. Kiselev and V. A. Cherepanov, Journal of Solid State Chemistry, 2010, 183, 1992 – 1997.

[33] E. Niwa, C. Uematsu, J. Mizusaki and T. Hashimoto, ECS Transactions, 2013, 57, 2133 – 2140.

the onset of LNF64 decomposition at around log(pO2, atm) = -3.3 and 1000°C. Therefore, we may expect that LNF64 is stable in air at temperatures even higher than 1000°C.

The authors clearly assume a hole to electron mobility ratio of 2 and then go on to describe this ratio as an experimental result, instead of supporting why they assumed this particular value. The authors need to rephrase their manuscript to provide support for the use of this ratio of 2 as an assumption (instead of the other way around).

We cannot agree with Referee 2. As it follows from the manuscript, the mobility ratio was found to be constant over complete temperature range investigated during the fitting procedure. It means that there was no a priori assignment *L* to 2 and that this value was obtained as a result of the fitting procedure for all temperatures investigated irrespective its initial approximation.

Oxygen nonstoichiometry, defect structure and related properties of $LaNi_{0.6}Fe_{0.4}O_{3-\delta}$

V.V. Sereda,* D.S. Tsvetkov, I.L. Ivanov and A.Yu. Zuev

Received Xth XXXXXXXXXX 20XX, Accepted Xth XXXXXXXXX 20XX
First published on the web Xth XXXXXXXXXX 200X
DOI: 10.1039/b000000x

Experimental results on oxygen nonstoichiometry (δ), thermal and chemical expansion ($\Delta L/L_0$), total electrical conductivity (σ) and Seebeck coefficient (Q) as functions of the oxygen partial pressure (p_{O_2}) and temperature for $LaNi_{0.6}Fe_{0.4}O_{3-\delta}$ are presented. The defect structure model of $LaNi_{0.6}Fe_{0.4}O_{3-\delta}$ based on the localized nature of the electronic defects was proposed and successfully verified using the measured $\delta = f(p_{O_2}, T)$ dependences. On the basis of the model proposed the concentrations of the point defects were calculated as functions of the T and p_{O_2}. These concentrations were then employed in the model of chemical expansion and that of Seebeck coefficient. It was shown that both models coincide completely with the corresponding experimental data. The chemical expansion coefficients (β_c) and mobilities of the charge carriers (electrons and holes) as functions of T and p_{O_2} were calculated as a result.

1 Introduction

Doped lanthanum nickelates are believed to be promising materials for the solid oxide fuel cells (SOFC) cathodes. It is known that undoped $LaNiO_{3-\delta}$ possesses high total conductivity even at room temperature but decomposes above 850 °C in air.[1] Partial substitution of Fe for Ni in $LaNi_{1-x}Fe_xO_{3-\delta}$ leads to a significant increase of the compound stability and, therefore, enables its applications in high-temperature devices. Chiba et al.[2] showed that $LaNi_{1-x}Fe_xO_{3-\delta}$ with $x = 0.4$ exhibits the highest electronic conductivity among all lanthanum nickelates doped with Fe. Furthermore, it was found that thermal expansion coefficient (TEC) of $LaNi_{0.6}Fe_{0.4}O_{3-\delta}$ is close to that of the yttrium-stabilized zirconia (YSZ), which is a state-of-the-art SOFC electrolyte. That is why $LaNi_{0.6}Fe_{0.4}O_{3-\delta}$ has been intensively studied and it has been shown to be the promising material not only as a SOFC cathode,[2–7] but as a current collector[8,9] and methane reforming catalyst.[10,11]

In order to understand better the possibilities and limitations of using $LaNi_{0.6}Fe_{0.4}O_{3-\delta}$ in various electrochemical devices it is crucial to know such properties as the total conductivity, thermoelectric power, chemical expansion, etc. depending on T and p_{O_2}. Reliable data on oxygen nonstoichiometry of this compound are strongly required because the oxygen content change may affect aforementioned properties significantly. It is also well-known that the defect structure of the oxide material is of a key importance for understanding of the behavior of solid oxide materials in different atmospheres at elevated temperatures.

It is necessary to note, however, that the results on oxygen nonstoichiometry,[12,13] thermal expansion[2,3,7,14,15] and electrical conductivity[2,12–14,16] of $LaNi_{0.6}Fe_{0.4}O_{3-\delta}$ available in literature seem to be controversial. For example, Niwa et al.[13] reported the values of oxygen nonstoichiometry in $LaNi_{0.6}Fe_{0.4}O_{3-\delta}$ lying in the span $0.09 \le \delta \le 0.11$ depending on p_{O_2} and T range $0.00 \ge \log(p_{O_2}, \text{atm}) \ge -3.65$ and $300 \le T, °\text{C} \le 700$, respectively. On the contrary, according to Chen et al.[12], δ in $LaNi_{0.6}Fe_{0.4}O_{3-\delta}$ does not exceed the value of 0.015 at 1000 °C and $\log(p_{O_2}, \text{atm}) = -3.75$, and Ohzeki et al.[15] reported that no mass loss was detected by thermogravimetric measurements up to 1000 °C for $LaNi_{0.6}Fe_{0.4}O_{3-\delta}$ sample in air. Almost equal slopes of δ vs. p_{O_2} dependences obtained by Niwa et al.[13] at different temperatures in the range 300-700 °C make their results somewhat doubtful. Indeed, it is well known for different perovskite compounds with small oxygen nonstoichiometry that slope of δ vs. p_{O_2} curves strongly depends on temperature (see, for example, Ref.[17]).

Decomposition of $LaNi_{0.6}Fe_{0.4}O_{3-\delta}$ was assumed in Ref.[13] to occur probably above 800 °C, which explains relatively low temperature range chosen for measurements of electrical conductivity and oxygen nonstoichiometry. Nevertheless, no evidence of such decomposition was presented by the authors.[13] On the contrary, it was shown in Refs.[15,18] that $LaNi_{0.6}Fe_{0.4}O_{3-\delta}$ is stable up to 1200 °C in air and at least up to 1100 °C at $\log(p_{O_2}, \text{atm}) = -1.5$, respectively.

The values of thermal expansion coefficient (α_T) of $LaNi_{0.6}Fe_{0.4}O_{3-\delta}$ reported by different authors are presented in Table 1. Despite the temperature ranges used in different works are very close to each other, α_T values differ signifi-

---

Department of Chemistry, Institute of Natural Sciences, Ural Federal University, Ekaterinburg, 620000, Russia. E-mail: vladimir.sereda@urfu.ru

cantly from one work to another.

Table 1 Thermal expansion coefficients of $LaNi_{0.6}Fe_{0.4}O_{3\text{-}\delta}$ reported by different authors

Reference	T (T range), °C	$\alpha_T \cdot 10^6$,K^{-1}
Chiba et al.[2]	20-800	11.2
Chiba et al.[2]	20-1000	11.4
Basu et al.[14]	700-900	11.8
Ohzeki et al.[15]	20-1000	12.4
Kammer et al.[3]	100-1000	13.4
Zhu et al.[7]	50-1000	14.5

As follows from Figs. 9 and Fig. 10 (see Section 3.4), where total electrical conductivity of $LaNi_{0.6}Fe_{0.4}O_{3\text{-}\delta}$ measured by different authors is given as a function of T and p_{O_2}, there is obvious discrepancy in such data reported. Despite there seems to be the influence of the synthesis route on electrical conductivity of $LaNi_{0.6}Fe_{0.4}O_{3\text{-}\delta}$,[14] it is difficult to explain huge difference between σ values reported by different authors taking into account only this circumstance. Dependence of δ on p_{O_2} for $LaNi_{0.6}Fe_{0.4}O_{3\text{-}\delta}$ remains still an open question since the former was measured only at a few values of the latter.[12,13] Thus the reliable data on oxygen nonstoichiometry and total conductivity of $LaNi_{0.6}Fe_{0.4}O_{3\text{-}\delta}$ as a function of temperature and oxygen partial pressure are still required.

Iwasaki et al.[19] reported the negative values of Seebeck coefficient for $LaNi_{0.6}Fe_{0.4}O_{3\text{-}\delta}$ in the temperature range 27-827 °C in air. However, for the oxide with $Q < 0$ total conductivity has to increase with decreasing oxygen partial pressure (or increasing δ) as the concentration of the electrons (as predominant charge carriers in the case of negative Q) increases. On the contrary, as it follows from the literature[12,13] and our measurements (see Fig. 10), σ dependences for $LaNi_{0.6}Fe_{0.4}O_{3\text{-}\delta}$ look like ones for a typical perovskite p-type conductor. As the negative values of Seebeck coefficient of $LaNi_{0.6}Fe_{0.4}O_{3\text{-}\delta}$ are in contradiction with the behavior of its total conductivity, the data of Iwasaki et al.[19] seem to be suspicious.

There are also some properties that were not discussed in the literature so far. Some authors reported an additional increase of TEC of $LaNi_{0.6}Fe_{0.4}O_{3\text{-}\delta}$ in the high-temperature region, as compared to linear trend estimated from the low temperature region.[14,15] In spite of the fact that this phenomenon can be attributed to the chemical expansion, there are no works devoted to estimation of a value of the chemical expansion coefficient. There are no data on the p_{O_2} dependence of Seebeck coefficient of $LaNi_{0.6}Fe_{0.4}O_{3\text{-}\delta}$. Moreover, the defect structure of $LaNi_{0.6}Fe_{0.4}O_{3\text{-}\delta}$ has not been studied yet.

Therefore, the priority purposes of this work were: (i) to obtain reliable data on oxygen nonstoichiometry of $LaNi_{0.6}Fe_{0.4}O_{3\text{-}\delta}$, (ii) to find an adequate model of its defect structure, (iii) to explore the possible relations between the defect structure and the properties of $LaNi_{0.6}Fe_{0.4}O_{3\text{-}\delta}$ such as chemical expansion and Seebeck coefficient.

2 Experimental

Powder sample of $LaNi_{0.6}Fe_{0.4}O_{3\text{-}\delta}$ was synthesized by means of the glycerol-nitrate method using the La_2O_3, $Ni(NO_3)_2 \cdot 6\,H_2O$ and $FeC_2O_4 \cdot 2\,H_2O$ as starting materials. All materials used had a purity of 99.99%. La_2O_3 was preliminary calcined at 1100 °C to remove absorbed H_2O and CO_2. Stoichiometric amounts of the precursors were dissolved in the concentrated nitric acid (99.99% purity) and the required volume of glycerol (99% purity) was added as a complexing agent and a fuel. Glycerol amount was calculated according to the reaction of the full reduction of all corresponding nitrates and the excess of HNO_3 to N_2. As prepared solution was heated continuously at 100 °C until complete water evaporation and pyrolysis of the dried precursor had occured. The resulting powder was subsequently fired in 3 steps at 900, 1000 and 1100 °C in air with intermediate regrindings to obtain the single phase $LaNi_{0.6}Fe_{0.4}O_{3\text{-}\delta}$. The X-ray diffraction (XRD) with the Equinox 3000 diffractometer (Inel, France) using Cu Kα radiation showed no indication for the presence of a second phase in $LaNi_{0.6}Fe_{0.4}O_{3\text{-}\delta}$ sample. Chemical composition of $LaNi_{0.6}Fe_{0.4}O_{3\text{-}\delta}$ was checked using ICP spectrometer ICAP 6500 DUO and atomic absorption spectrometer Solaar M6, Thermo Scientific, USA. $LaNi_{0.6}Fe_{0.4}O_{3\text{-}\delta}$ sample was shown to have the stoichiometric cation composition within the accuracy of 2%.

For the measurements of thermal and chemical expansion, electrical conductivity and Seebeck coefficient single phase powder of $LaNi_{0.6}Fe_{0.4}O_{3\text{-}\delta}$ was axially pressed into rectangular bars of $30 \times 4 \times 4$ mm^3 at 40 MPa and sintered at 1200 °C for 24 h in air. Due to the small size of a coulometric cell, one of the $LaNi_{0.6}Fe_{0.4}O_{3\text{-}\delta}$ sample bars obtained accordingly was cut in half length to be used for the coulometric titration experiment. The relative density of the sample bars used for the coulometric titration, dilatometric and electrical conductivity measurements was found to be higher than 95%.

The change of oxygen nonstoichiometry with T and p_{O_2} was measured by the coulometric titration technique. The original coulometric titration set up and technique are described in detail elsewhere.[20]

The coulometric titration experiment was carried out in two modes. In the first mode at constant T we stepwise pumped the oxygen in or out of the coulometric cell passing known constant current through the solid YSZ electrolyte. Each titration step is followed by the relaxation of the sample when one comes to equilibrium state at new p_{O_2} and given T. Oxygen nonstoichiometry change is calculated at each titration step according to the following equation:

$$\Delta\delta = \frac{2M}{m}\left[\frac{Q}{4F} - \frac{V}{RT}\left(p_{O_2}^{(0)} - p_{O_2}^{(1)}\right)\right], \qquad (1)$$

where M, m, Q, F, V, T, $p_{O_2}^{(0)}$, $p_{O_2}^{(1)}$, 4 and R are the molar mass of the oxide investigated (g/mol), oxide sample mass (g), electric charge passed through the coulometric titration cell (C), Faraday constant (C/mol), free volume of the coulometric cell (m^3), temperature (K), oxygen partial pressure before titration (Pa), oxygen partial pressure after titration (Pa), number of electrons taking part in the electrode reaction, and universal gas constant (J/(mol·K)), respectively.

In the second mode starting from initial $p_{O_2}^{(0)}$ a stepwise changes in T were applied. From observed changes in oxygen partial pressure one can easily calculate a δ change caused by temperature variation:

$$\Delta\delta = \delta_1 - \delta_0 = \frac{2mV\left(\frac{p_{O_2}^{(1)}}{T_1} - \frac{p_{O_2}^{(0)}}{T_0}\right)}{MR}. \qquad (2)$$

The absolute value of δ in $LaNi_{0.6}Fe_{0.4}O_{3-\delta}$ was determined by the direct reduction of the oxide sample by H_2 flux in the thermogravimetric (TG) set up (TG/H_2) using STA 409 PC Luxx (Netzsch GmbH, Germany) thermobalance. The results of TG/H_2 showed that the absolute oxygen content in $LaNi_{0.6}Fe_{0.4}O_{3-\delta}$ at 750 °C in air is equal to 3.00 ± 0.01. Such a small value of δ in air is in agreement with the literature data.[12,15]

Isobaric thermal expansion measurements in air were carried out using a DIL 402C (Netzsch GmbH, Germany) dilatometer in the temperature range from room temperature to 1100 °C with heating/cooling rate 5 °C/min and air flow rate 50 ml/min. Chemical expansion as a function of p_{O_2} was studied using the original dilatometric set up which has been described in details elsewhere.[21] This set up is equipped with YSZ oxygen sensor placed in close vicinity to the sample to perform accurate simultaneous measurement of the sample elongation or contraction, temperature and oxygen partial pressure. Typical results of such measurements are presented in Fig. 1, where a relaxation curve is given along with the equilibrated values of the sample length.

Total conductivity and Seebeck coefficient were measured simultaneously vs. T and p_{O_2} using the conventional 4-probe technique.

3 Results and discussion

3.1 Oxygen nonstoichiometry of $LaNi_{0.6}Fe_{0.4}O_{3-\delta}$

Experimental data on the oxygen nonstoichiometry of $LaNi_{0.6}Fe_{0.4}O_{3-\delta}$ obtained by coulometric titration technique are shown in Fig. 2. During the coulometric titration experiment oxygen was stepwise pumped out of the titration cell and then pumped in. Thus the curves going from low to high oxygen partial pressure and vice versa were obtained. These data are presented in Fig. 2 showing good reproducibility and reversibility of the coulometric titration results.

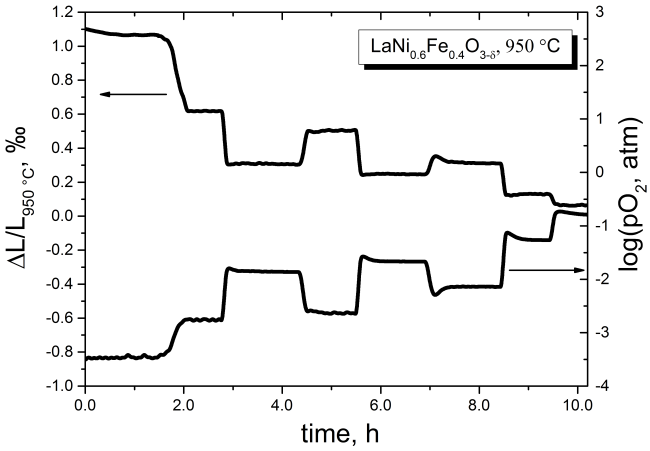

Fig. 1 Raw trace of isothermal expansion of the $LaNi_{0.6}Fe_{0.4}O_{3-\delta}$ sample length (L) depending on time and p_{O_2}

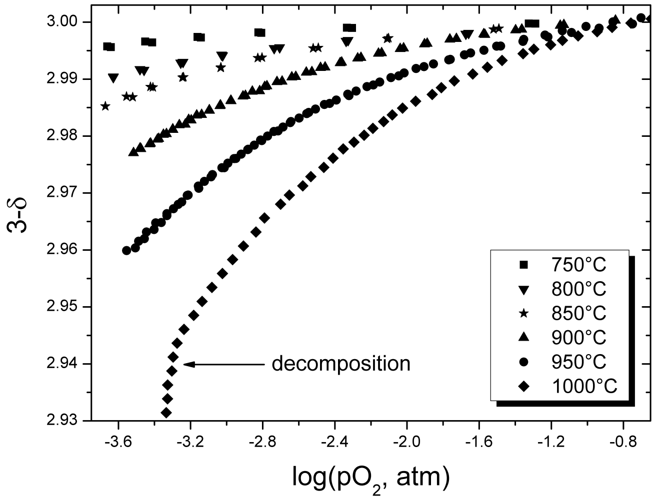

Fig. 2 Oxygen nonstoichiometry of $LaNi_{0.6}Fe_{0.4}O_{3-\delta}$ at different temperatures

It can be noted that obtained values of δ are significantly lower than those reported by Niwa et al.[13] but they are about the same order of magnitude as the data given by Chen et al.[12] Steep change in δ at around $\log(p_{O_2}, \text{atm}) = -3.3$ and 1000 °C can be related to the beginning of the sample decomposition. The relatively low stability limit of $LaNi_{0.6}Fe_{0.4}O_{3-\delta}$ at 1000 °C is not surprising as Kiselev et al.[18] reported that

$LaNi_{0.6}Fe_{0.4}O_{3\text{-}\delta}$ phase is stable only up to $\log(p_{O_2}, \text{atm}) = -1.5$ at 1100 °C. Therefore properties of $LaNi_{0.6}Fe_{0.4}O_{3\text{-}\delta}$ measured at lower p_{O_2} and higher temperatures seem to be doubtful. For example, Chen et al.[12] found that it is impossible to obtain stable values of the oxygen content and conductivity of $LaNi_{0.6}Fe_{0.4}O_{3\text{-}\delta}$ at 1000 °C and $\log(p_{O_2}, \text{atm}) = -3.75$, although they have not detected any phase except $LaNi_{0.6}Fe_{0.4}O_{3\text{-}\delta}$ after its treatment under these conditions for 20 h.

3.2 Defect structure analysis of $LaNi_{0.6}Fe_{0.4}O_{3\text{-}\delta}$

It is known that the defect structure of the perovskites depends strongly on the nature of the charge carriers (electrons and electron holes), which could be either localized (*e.g.* on the *3d*-metals, $Me_{Me}^{/}$ and $Me_{Me}^{\bullet}$) or delocalized ($e^{/}$ and $h^{\bullet}$). Thereby we can speak about the small or large polaron hopping conduction mechanism in case of localized or delocalized charge carriers, accordingly.

It should be taken into account that the topic of the transport mechanism for perovskite materials still remains controversial. Sometimes so-called "pseudometallic" character of conductivity when total conductivity of a substance decreases with increasing temperature is referred to the delocalized charge carrier approach. Nevertheless, for example, for $LaCoO_3$ high value and negative temperature coefficient of total conductivity (similar behavior is observed for $LaNi_{0.6}Fe_{0.4}O_{3\text{-}\delta}$) were found to be quite consistent with small polaron mechanism of conductivity at high temperatures when activation energy for hole hopping is small and hole's mobility has typical value for a small polaron carrier.[22] Furthermore, it was found that for undoped and various doped $LaCoO_3$ better explanation of available experimental data on the defect-induced properties can be given on the basis of the existence of small polarons on the cobalt sites.[23] There is also an example of the lanthanum ferrite doped with Ni, $LaNi_{0.3}Fe_{0.7}O_{3\text{-}\delta}$, for which it was found that its defect structure "can be described in terms of randomly distributed point defects within a small polaron concept of electronic defect state."[17] Taking into account all mentioned above, we can consider the charge carriers in $LaNi_{0.6}Fe_{0.4}O_{3\text{-}\delta}$ to be localized.

The undoped $LaNiO_3$ was chosen as a reference crystal in order to define lattice constituents and point defects in $LaNi_{0.6}Fe_{0.4}O_{3\text{-}\delta}$ using the Kröger-Vink notation. Therefore, we can propose the simple point defect model in which predominant defect species are supposed to be $V_O^{\bullet\bullet}$, $Ni_{Ni}^{/}$ and $Fe_{Ni}^{\bullet}$. The reasons for assuming that elecrons are localized on Ni and holes - on Fe are given below.

Within the framework of this defect structure model, the oxygen exchange reaction between $LaNi_{0.6}Fe_{0.4}O_{3\text{-}\delta}$ and the ambient gas phase can be represented by

$$O_O^{\times} + 2Ni_{Ni}^{\times} \rightleftarrows \frac{1}{2}O_2 + V_O^{\bullet\bullet} + 2Ni_{Ni}^{/}. \tag{3}$$

Two kinds of disproportionation between the Fe ions can be proposed: the disproportionation of Fe^{3+} to Fe^{2+} and Fe^{4+}, and one of Fe^{4+} to Fe^{3+} and Fe^{5+}. However, the former reaction in acceptor-doped $LaFeO_3$ was found to be unfavorable,[24] and the latter was found in some perovskite ferrites only at temperatures lower than 300 K,[25–28] which is obviously out of the scope of our work. Taking into account that there are evidences for the presence of the Fe^{4+} ions in $LaNi_{1\text{-}x}Fe_xO_{3\text{-}\delta}$,[17,29,30] and that Ni is more electronegative element as compared to Fe, charge disproportionation in $LaNi_{0.6}Fe_{0.4}O_{3\text{-}\delta}$ can be given by the following reaction:

$$Fe_{Ni}^{\times} + Ni_{Ni}^{\times} \rightleftarrows Fe_{Ni}^{\bullet} + Ni_{Ni}^{/}, \tag{4}$$

Equilibrium constants of the proposed defect reactions along with equations of mass balance and electroneutrality form the following set of nonlinear equations:

$$\begin{cases} K_3 = \dfrac{p_{O_2}^{1/2} \cdot [V_O^{\bullet\bullet}] \cdot [Ni_{Ni}^{/}]^2}{[O_O^{\times}] \cdot [Ni_{Ni}^{\times}]^2} = K_3^0 \cdot \exp\left(-\dfrac{\Delta H_3}{RT}\right) \\ K_4 = \dfrac{[Fe_{Ni}^{\bullet}] \cdot [Ni_{Ni}^{/}]}{[Fe_{Ni}^{\times}] \cdot [Ni_{Ni}^{\times}]} = K_4^0 \cdot \exp\left(-\dfrac{\Delta H_4}{RT}\right) \\ [O_O^{\times}] = 3 - \delta \\ \delta = [V_O^{\bullet\bullet}] \\ [Ni_{Ni}^{\times}] + [Ni_{Ni}^{/}] = 0.6 \\ [Fe_{Ni}^{\times}] + [Fe_{Ni}^{\bullet}] = 0.4 \\ [Ni_{Ni}^{/}] = 2[V_O^{\bullet\bullet}] + [Fe_{Ni}^{\bullet}] \end{cases} \tag{5}$$

The analytical solution of this set of equations yields the model function

$$P_{O_2}^{1/4} = -A \cdot \frac{-K_4 + 6 + 10K_4\delta - 10\delta - B}{5K_4 + 10K_4\delta - 10\delta - B}, \tag{6}$$

where
$A = \sqrt{K_3(3-\delta)/\delta}$
and
$B = \sqrt{K_4^2(1 - 20\delta + 100\delta^2) + K_4(24 - 200\delta^2) + 100\delta^2}$.
Since the oxygen nonstoichiometry of $LaNi_{0.6}Fe_{0.4}O_{3\text{-}\delta}$ was measured in the relatively narrow temperature range, we can assume that the enthalpies of the defect reactions are constant. This allows to substitute the equilibrium constants in Eq. 6 by their temperature dependences (see Eq. 5) and then to fit the Eq. 6 to the experimental data on the $LaNi_{0.6}Fe_{0.4}O_{3\text{-}\delta}$ oxygen nonstoichiometry. The results of the least square fitting are presented in Fig. 3 and the Table 2. As seen, there is a good

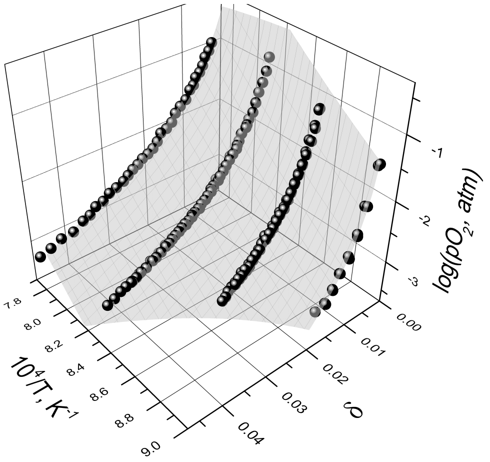

Fig. 3 Results of the nonlinear surface fitting of the defect structure model Eq. 6 for $LaNi_{0.6}Fe_{0.4}O_{3-\delta}$. Points - experimental data, surface - fitted model

Table 2 The fitting parameters of the defect structure model analysis

Defect reaction, Eq.	ΔH_i, kJ/mol	$\ln K_i^0$	R^2
3	85.576	0.807	0.996
4	-159.695	-14.614	

agreement between calculated and measured nonstoichiometry values.

The values of the fitted parameters are summarized in Table 2. The error for the fitted parameters was relatively low and did not exceed 10%. During the fitting procedure several sets of initial values of the fitting parameters were used and in all cases fitting procedure was stable and converged to the same values of the fitting parameters within the error range mentioned above. These values allow to calculate the concentrations of all point defects as functions of temperature and oxygen partial pressure (or oxygen nonstoichiometry). Concentrations of $Ni_{Ni}^{/}$ and $Fe_{Ni}^{\bullet}$ calculated accordingly are plotted in Fig. 4. As seen, concentration of the $Fe_{Ni}^{\bullet}$ decreases and that of $Ni_{Ni}^{/}$ - increases with the increase of δ in $LaNi_{0.6}Fe_{0.4}O_{3-\delta}$ at a given temperature. Negative value of the enthalpy ΔH_4 of the charge disproportionation reaction causes the decrease of the concentrations of charged defect species $Ni_{Ni}^{/}$ and $Fe_{Ni}^{\bullet}$ with increasing temperature, as seen in Fig. 4.

3.3 Thermal and chemical expansion of $LaNi_{0.6}Fe_{0.4}O_{3-\delta}$

Chemical expansion of $LaNi_{0.6}Fe_{0.4}O_{3-\delta}$ normalized to the length of the sample with $\delta = 0$ at a given temperature is shown in Fig. 5 as a function of the oxygen partial pressure.

The chemical expansion was modeled using the approach

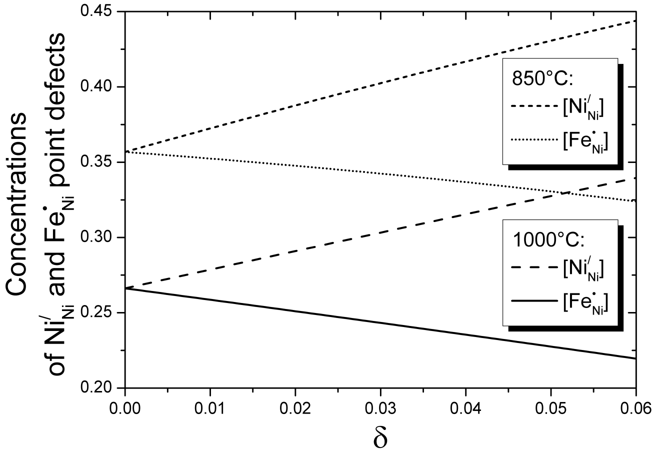

Fig. 4 Concentrations of $Ni_{Ni}^{/}$ and $Fe_{Ni}^{\bullet}$ vs. δ at different temperatures, calculated according to the defect structure model of $LaNi_{0.6}Fe_{0.4}O_{3-\delta}$

described in our previous works.[21,31–35] In this approach it is assumed that the main reason for the chemical expansion is the relative change of the average ionic radii. This change in radii occurs as a result of the 3d-metal reduction/oxidation due to the release/uptake of the oxygen by the oxide lattice. Using the assumption of the isotropic expansion and describing the oxide crystal structure as a closely packed lattice formed by rigid spheres of ions, chemical expansion can be calculated by using the following equation:

$$\frac{\Delta L}{L_0} = \frac{\sum\limits_i \left(c_i r_i - c_{i_0} r_i\right)}{\sum\limits_i c_{i_0} r_i}, \tag{7}$$

where c_i and r_i are the concentration and ionic radius of the i-th ion of the oxide, and the index 0 corresponds to the reference state with known oxygen nonstoichiometry (*e.g.* $\delta = 0$) at a given temperature. Using the given approach it is possible to obtain theoretical dependences $\Delta L/L_0 = f(T, \delta)$ simply by substituting the concentrations and radii of the ionic species to Eq. 7. Corresponding concentrations can be easily obtained using the defect structure model proposed and verified above. Crystal ionic radii given by Shannon[36] can be used as r_i, taking into account the corresponding coordination numbers ($CN_{La} = 12$, $CN_{Ni} = CN_{Fe} = CN_O = 6$) with respect to the crystal structure of $LaNi_{0.6}Fe_{0.4}O_{3-\delta}$.

However, one should decide in which spin state Fe^{3+} ions occur since their ionic radii depend on their spin state similar to the Co ions.[36] In our previous works[32–35] we have already proposed the gradual transition from low (LS) to high (HS) spin state for Co^{3+} in different doped lanthanum cobaltites and found that this approach is quite consistent with the chemical expansion behavior observed for them.[32–35] Moreover, mag-

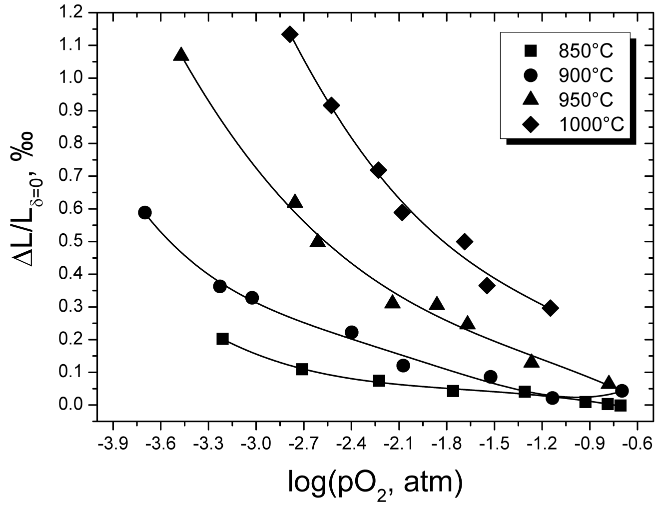

Fig. 5 Chemical expansion of $LaNi_{0.6}Fe_{0.4}O_{3-\delta}$ as a function of p_{O_2} normalized as described in the text. Symbols - experimental data, lines - for eye guide only

netic moment of $La_{0.8}Sr_{0.2}CoO_{3-\delta}$ calculated at 1164 K on the basis of the spin distribution obtained for different cobalt species[32] comes to value of 4.05 μB while that is 3.8 μB according to Baskar and Adler[37], who calculated the latter from *in situ* high-temperature measurements of the magnetic susceptibility. Furthermore, Baskar and Adler showed that magnetic moment of $La_{0.8}Sr_{0.2}CoO_{3-\delta}$ does not depend on its oxygen nonstoichiometry in practical term. This was the case for the magnetic moment calculated by us.[32] The evidence of such gradual transition from low to high-spin state for Fe^{3+} in perovskite oxides was shown by Feldhoff et al.[38] Thus, assuming similar behavior for Fe^{3+} in $LaNi_{0.6}Fe_{0.4}O_{3-\delta}$, we can define the mean ionic radius of Fe^{3+} as weighted sum of its radii in low and high spin states:

$$r_{Fe^{3+}} = x^{HS}_{Fe^{3+}} \cdot r^{HS}_{Fe^{3+}} + x^{LS}_{Fe^{3+}} \cdot r^{LS}_{Fe^{3+}}, \tag{8}$$

where $x^{HS}_{Fe^{3+}}$ and $x^{LS}_{Fe^{3+}} = 1 - x^{HS}_{Fe^{3+}}$ are the fractions of the high-spin and low-spin Fe^{3+} ions, accordingly.

For some reason, the existence of the low-spin Fe^{3+} in perovskites is regarded by some scientists as extremely doubtful. It should be noted here that there is no information in literature about in situ high-temperature measurements which could confirm or disprove that Fe^{3+} in $LaNi_{0.6}Fe_{0.4}O_{3-\delta}$ is always in high-spin state. Furthermore, it is known that in order to obtain the spin states, for example, from the Mössbauer spectra, the fitting procedure must be involved. In this respect, it is worth noting that the similar Mössbauer spectra obtained for the similar compounds, $PrFe_{1-x}Ni_xO_3$ ($x \leq 0.3$)[39] and $LaNi_{1-x}Fe_xO_{3-\delta}$ (x=0-0.5),[40] were interpreted in the completely different ways. While Fe^{3+} in the $PrFe_{1-x}Ni_xO_3$ was assumed to be in the mixed-spin state,[39] the presence of the low-spin Fe^{3+} in $LaNi_{1-x}Fe_xO_{3-\delta}$ was ruled out[40] - in either case on the basis of the fitting procedure. Therefore the real spin state of iron in perovskites at high and intermediate temperatures should be addressed in further investigations.

Nevertheless, based on the available data, we can assume that Fe^{3+} exists in perovskite oxides in the low-spin state,[39] and that transition from low to high-spin state occurs with increasing temperature.[38] Moreover, Fig. 6, where the chemical expansion is given as a function of oxygen nonstoichiometry at a given temperature, is in favour of high-temperature spin-state transition for Fe^{3+} in $LaNi_{0.6}Fe_{0.4}O_{3-\delta}$. Indeed, as seen the chemical expansion measured at 950 °C exceeds the one measured at 900 °C at the same value of the oxygen nonstoichiometry. This behavior cannot be explained by an influence of the temperature dependence of the equilibrium constant, K_4, of charge disproportionation reaction Eq. 4, since the one is negative as follows from Table 2 and, therefore, would lead contrariwise.

In principle, Ni^{3+} ions can exist in different spin states as well. In this respect, the reasons for excluding Ni^{3+} spin-state transition from the consideration in the chemical expansion model should be pointed out explicitly. First of all, the data on the LS-HS transition for the Ni^{3+} ions are absent in the literature. Then, the difference in crystal radii for 6-coordinated HS and LS Fe^{3+} is (0.785-0.69)=0.095 Å which is more than two times greater than that for Ni^{3+}: (0.74-0.7)=0.04 Å.[36] Therefore, it can be concluded that the ionic radii for high- and low-spin Ni^{3+} are close to each other. In reality, it seems to be almost impossible to detect the spin state transition for Ni^{3+}, even if one exists, by means of the dilatometric measurements. Finally, it can be shown that the introduction of the Ni^{3+} spin-state transition to $LaNi_{0.6}Fe_{0.4}O_{3-\delta}$ chemical expansion model instead of (or even along with) such for the Fe^{3+} ions influences the shape of the theoretically calculated curve insignificantly. Therefore, one can conclude that the overcomplication of the chemical expansion model caused by the consideration of Ni^{3+} spin-state transition is not justified.

Substitution of Eq. 8 in Eq. 7 leads to the theoretical function $\Delta L/L_0 = f(T, \delta, x^{HS}_{Fe^{3+}})$ in which the only unknown parameter is $x^{HS}_{Fe^{3+}}$. Eq. 7 was fitted to the experimental data on chemical expansion of $LaNi_{0.6}Fe_{0.4}O_{3-\delta}$. The results of this fit are presented in Fig. 6. The values of $x^{HS}_{Fe^{3+}}$ obtained as a result of the fitting procedure are plotted in Fig. 7 showing the expected increase of the high spin Fe^{3+} fraction with temperature.

Thermal expansion of $LaNi_{0.6}Fe_{0.4}O_{3-\delta}$ measured in air is shown in Fig. 8. α plotted in the same figure as a dash line is an “apparent” TEC defined as:

$$\alpha = \frac{1}{L_0}\left(\frac{\Delta L}{\Delta T}\right). \tag{9}$$

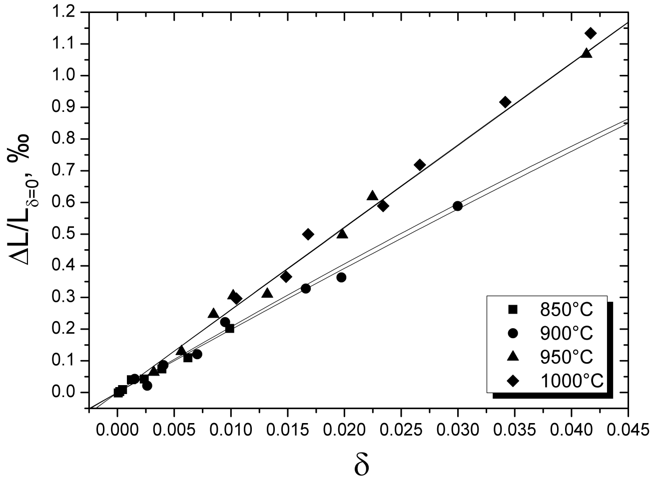

Fig. 6 Chemical expansion of $LaNi_{0.6}Fe_{0.4}O_{3-\delta}$ as a function of oxygen nonstoichiometry. The symbols represent the experimental data while lines correspond to the values calculated according to the Eq. 7

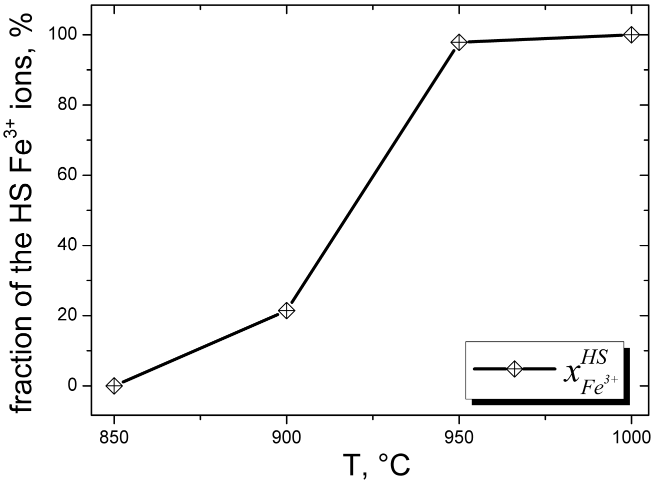

Fig. 7 Calculated fraction of the high spin (HS) Fe^{3+} ions in $LaNi_{0.6}Fe_{0.4}O_{3-\delta}$ vs. temperature. Line is given for eye guide only

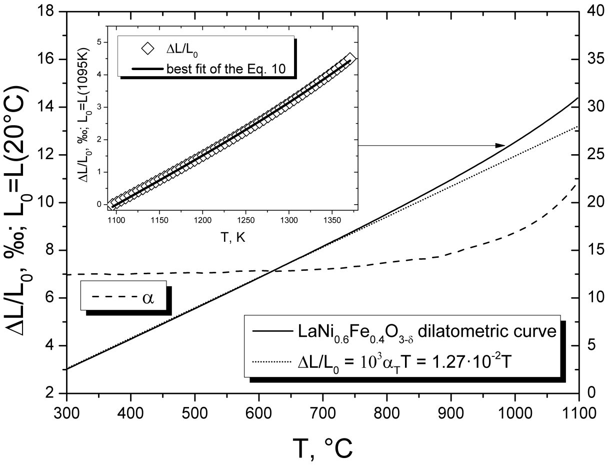

Fig. 8 Dilatometric curve of $LaNi_{0.6}Fe_{0.4}O_{3-\delta}$ in air

The average thermal expansion coefficient of $LaNi_{0.6}Fe_{0.4}O_{3-\delta}$ in the temperature range 200-750 °C was found to be $12.7 \cdot 10^{-6}$ K^{-1}. The dotted line in Fig. 8 corresponds to the contribution of the thermal expansion to overall one. As seen it coincides perfectly with the low-temperature region of the dilatometric curve, while there is obvious positive deviation of the latter from the linear trend in high-temperature region. Such deviation is typical for the perovskite materials which undergo isothermal (chemical) expansion. The observed deviation corresponds to the contribution of the chemical expansion to the overall one, which, therefore, can be represented by the following equation:

$$\Delta L/L_0 = \alpha_T\,(T - T_0) + \beta_c\,(\delta(T) - \delta_0)\,, \qquad (10)$$

where α_T is TEC, L_0 is the sample length at T_0 and δ_0, and β_c is the chemical expansion coefficient which is often used for characterization of the chemical expansivity of materials.[41] Results of the fitting procedure are shown in Fig. 8, and fitted value of β_c is presented in Table 3. It follows from Table 3 that the mean value of β_c calculated using the dilatometric curve in air can be used only for estimation of the magnitude of chemical expansion as it does not reflect completely the expansion of the sample at a given temperature.

3.4 Electrical conductivity and Seebeck coefficient of $LaNi_{0.6}Fe_{0.4}O_{3-\delta}$

Experimental data on the conductivity of $LaNi_{0.6}Fe_{0.4}O_{3-\delta}$ vs. temperature and oxygen partial pressure are shown in Figs. 9 and 10. It has been already mentioned in the introduction that there is a huge discrepancy between the experimental data obtained by different authors. However, our data on the total conductivity of $LaNi_{0.6}Fe_{0.4}O_{3-\delta}$ seem to be consistent with some of those presented earlier.[12,14]

Fig. 11 shows isothermal dependences of Seebeck coefficient on oxygen nonstoichiometry. Positive values of Q along with the σ decrease upon p_{O_2} lowering indicate in favor of p-type semiconducting behavior of $LaNi_{0.6}Fe_{0.4}O_{3-\delta}$. Taking into account the data on $LaNi_{0.6}Fe_{0.4}O_{3-\delta}$ oxygen diffusion coefficient,[42] one can conclude that oxygen ionic conductivity of $LaNi_{0.6}Fe_{0.4}O_{3-\delta}$ should be lower than the electronic one by several orders of magnitude. Therefore, we can assume that the major charge carriers are the electronic defects. Thus, See-

Table 3 Chemical expansion coefficients of $LaNi_{0.6}Fe_{0.4}O_{3-\delta}$

T (T range), °C	β_c	R^2	comment
820-1100	0.0231	0.9996	calculated using Eq. 10 from the results of the dilatometric measurements in air
1000	0.0269	0.9898	isothermal measurements at different p_{O_2}
950	0.0261	0.9925	
900	0.0195	0.9876	
850	0.0196	0.9840	

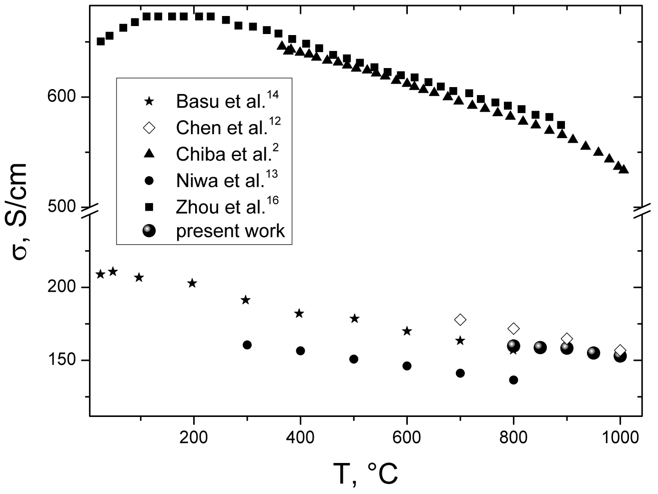

Fig. 9 Total conductivity of $LaNi_{0.6}Fe_{0.4}O_{3-\delta}$ as a function of T in air in comparison with the literature data

beck coefficient of $LaNi_{0.6}Fe_{0.4}O_{3-\delta}$ can be given by[22,43]

$$Q_t = \frac{[Ni^{/}_{Ni}]Q_e + L[Fe^{\bullet}_{Ni}]Q_h}{[Ni^{/}_{Ni}] + L[Fe^{\bullet}_{Ni}]}, \qquad (11)$$

where Q_e and Q_h are partial thermoelectric coefficients of electrons and holes, and $L = U_h/U_e$ is a ratio of their mobilities. According to Heikes,[44] Q_e and Q_h can be expressed as:

$$Q_h = \frac{k}{|e|}\left[\ln\left(\frac{[Fe^{\times}_{Ni}]}{[Fe^{\bullet}_{Ni}]}\right) + \frac{S^*_h}{k}\right] \qquad (12)$$

and

$$Q_e = -\frac{k}{|e|}\left[\ln\left(\frac{[Ni^{\times}_{Ni}]}{[Ni^{/}_{Ni}]}\right) + \frac{S^*_e}{k}\right], \qquad (13)$$

where k is a Boltzmann constant, e - elementary charge, $S^*_i = H^*_i/T$ and H^*_i are the entropy and enthalpy of holes (for $i \equiv h$) or electrons ($i \equiv e$) transport, respectively.

Substitution of the corresponding defect concentrations calculated using the defect structure model proposed above to the Eq. 11 allows to obtain the theoretical function $Q_t = f(\delta, L, S^*_h, S^*_e)_T$, which can be fitted to the experimental isothermal dependences $Q_t = f(\delta)$. Results of the least square fitting are summarized in Table 4 and shown in Fig. 11 along with the experimental data. As seen, there is an excellent agreement between calculated and measured values. It can be mentioned that the electron and hole transport entropy values are very close to each other and they decrease with increasing temperature, while L is found to be constant over all temperature range investigated.

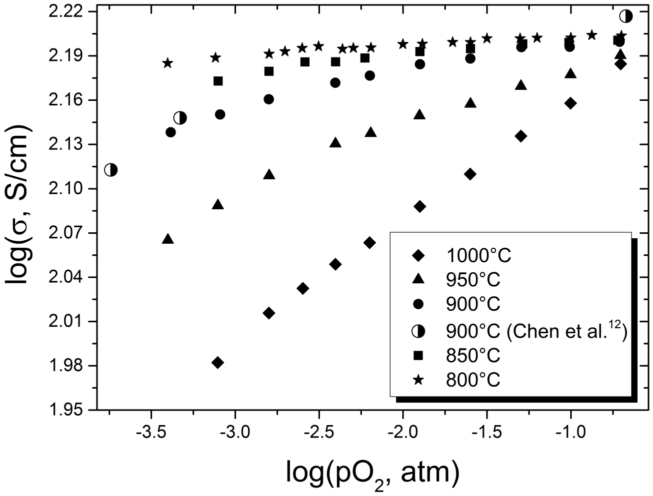

Fig. 10 Total conductivity of $LaNi_{0.6}Fe_{0.4}O_{3-\delta}$ as a function of T and p_{O_2}

Table 4 The fitting results of the Seebeck coefficient model analysis

T, °C	$L = U_h/U_e$	S^*_e, 10^{-4} eV/K	S^*_h, 10^{-4} eV/K	R^2
1000	2.00	1.58	1.68	0.9875
950	2.00	2.45	2.32	0.9927
900	2.00	3.50	3.13	0.9945
850	2.00	4.49	3.98	0.9573

Total conductivity σ_t of $LaNi_{0.6}Fe_{0.4}O_{3-\delta}$, neglecting the small contribution of the oxygen ions to the overall charge transfer, can be expressed as

$$\begin{aligned}\sigma_t &= \frac{a|e|}{V_c}\left(U_e[Ni^{/}_{Ni}] + U_h[Fe^{\bullet}_{Ni}]\right) = \\ &= \frac{a|e|}{V_c}U_e\left([Ni^{/}_{Ni}] + L[Fe^{\bullet}_{Ni}]\right),\end{aligned} \qquad (14)$$

where a, V_c, U_e and U_h are the number of the formula units of $LaNi_{0.6}Fe_{0.4}O_{3-\delta}$ per unit cell, the volume of the unit cell and the mobilities of electrons and holes, respectively. For the $LaNi_{0.6}Fe_{0.4}O_{3-\delta}$ with $R\bar{3}c$ space group $a = 6$ and $V_c = 360.0826$ Å at 900 °C.[12] Substitution of the fitted L values to

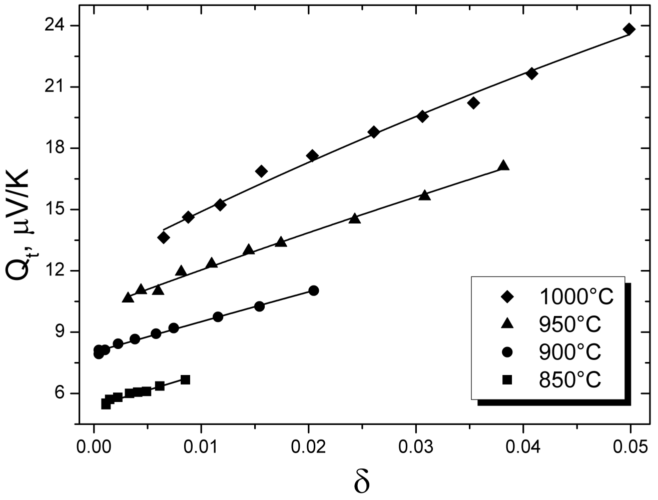

Fig. 11 Seebeck coefficient of $LaNi_{0.6}Fe_{0.4}O_{3-\delta}$ vs. oxygen nonstoichiometry. Lines correspond to the best fit of the function Eq. 11

the Eq. 14 allows to obtain the equations for the electrons and holes mobilities using the measured total conductivity data. U_e and U_h values calculated accordingly are plotted in Fig. 12 as functions of δ showing the typical values for the small polaron hopping. Despite the concentration of the holes is lower than that of the electrons, as shown in Fig. 4, the mobilities of the holes exceeds those of the electrons in the whole temperature range investigated. For this reason, holes remain the predominant charge carriers in $LaNi_{0.6}Fe_{0.4}O_{3-\delta}$ over complete oxygen nonstoichiometry range. Since $LaNi_{0.6}Fe_{0.4}O_{3-\delta}$ is a p-type semiconductor and its total conductivity increases with the concentration of holes, it is not surprising that $U_e < U_h$. Quite remarkable observation follows from comparison of Figs. 4 and 12, since the concentration of holes decreases with temperature while their mobility increases.

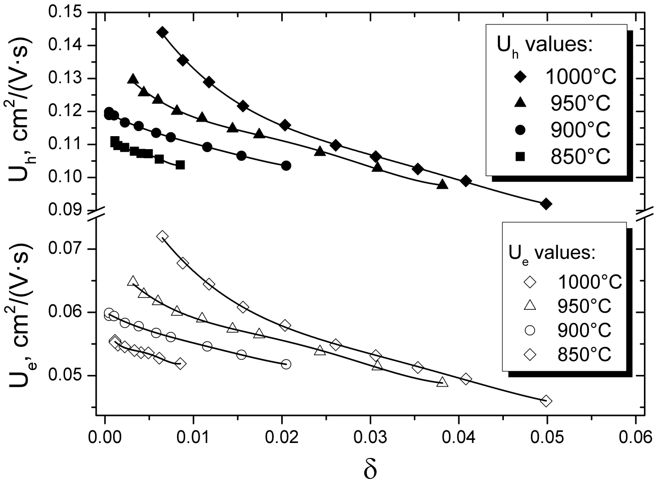

Fig. 12 Mobilities of the localized electrons and holes in $LaNi_{0.6}Fe_{0.4}O_{3-\delta}$ as functions of δ at different temperatures

In the work of Niwa et al.[13] the hole mobility in $LaNi_{0.6}Fe_{0.4}O_{3-\delta}$ was found to be $U_h = 0.257$ $cm^2V^{-1}s^{-1}$. It was calculated for the oversimplified case where U_h is treated as independent of temperature and holes are the only charge carriers. Nevertheless, despite the obvious errors related to these simplifications, U_h value obtained in Ref.[13] has the same order of magnitude as the ones calculated in the present work.

Values of the U_h and U_e reported by Kiselev et al.[17] for $LaNi_{0.3}Fe_{0.7}O_{3-\delta}$ are several times higher than those found in this work for $LaNi_{0.6}Fe_{0.4}O_{3-\delta}$. It should be mentioned here that $LaNi_{0.3}Fe_{0.7}O_{3-\delta}$ has the total conductivity, values of which are similar to those of $LaNi_{0.6}Fe_{0.4}O_{3-\delta}$, and higher values of the Seebeck coefficient while its charged point defect concentrations are several times lower than those of $LaNi_{0.6}Fe_{0.4}O_{3-\delta}$ at the same T and δ. However, Kiselev et al.[17] completely neglected the transport entropy S_i^* and introduced spin degeneracy factors to the Heikes formula in order to treat the Seebeck coefficient data of $LaNi_{0.3}Fe_{0.7}O_{3-\delta}$. Thus, the reason for the higher mobility of electrons and holes found in Ref.[17] for $LaNi_{0.3}Fe_{0.7}O_{3-\delta}$ as compared to our results on $LaNi_{0.6}Fe_{0.4}O_{3-\delta}$ can be attributed to the difference in the U_h and U_e calculation approaches.

4 Conclusions

Oxygen nonstoichiometry of $LaNi_{0.6}Fe_{0.4}O_{3-\delta}$ was studied as a function of temperature and oxygen partial pressure in the ranges $-3.5 \leq \log(p_{O_2}, \mathrm{atm}) \leq -0.7$ and $750 \leq T, °C \leq 1000$. It was found that δ does not exceed 0.06 over the whole T and p_{O_2} range investigated. The defect structure model of $LaNi_{0.6}Fe_{0.4}O_{3-\delta}$ was proposed and successfully verified using the experimental data on δ as a function of T and p_{O_2}. As a result, corresponding equilibrium constant values were found, allowing to calculate the point defect concentrations at a given T and p_{O_2}. Concentrations of defect species calculated accordingly were used for the computation of chemical expansion and electrotransport properties of $LaNi_{0.6}Fe_{0.4}O_{3-\delta}$.

Thermal expansion coefficient of $LaNi_{0.6}Fe_{0.4}O_{3-\delta}$ was found to be $12.7 \cdot 10^{-6}$ K^{-1} in the temperature range 200-750 °C. Chemical expansion of $LaNi_{0.6}Fe_{0.4}O_{3-\delta}$ was investigated by means of both isothermal and isobaric dilatometric experiments. Values of the chemical expansion coefficient calculated as a result lie in range $0.0195 \leq \beta_c \leq 0.0269$ at $850 \leq T, °C \leq 1000$. β_c of $LaNi_{0.6}Fe_{0.4}O_{3-\delta}$ was found to increase with temperature. This phenomenon is believed to be related to the temperature-induced spin-state transition of the Fe^{3+} ions from low to high spin state.

Total conductivity and Seebeck coefficient of $LaNi_{0.6}Fe_{0.4}O_{3-\delta}$ were measured as a functions of T and p_{O_2}. Electron holes were shown to be the predominant charge carriers in $LaNi_{0.6}Fe_{0.4}O_{3-\delta}$.

Both the chemical expansion and Seebeck coefficient were successfully described on the basis of the proposed defect structure model. It is shown that experimental values and those calculated are in the good agreement with each other. Mobilities of the charged defect species were calculated using the data on σ of $LaNi_{0.6}Fe_{0.4}O_{3-\delta}$ and the results of the Seebeck coefficient modeling. It was found that the concentration of holes is lower than that of electrons in the whole T and p_{O_2} ranges investigated, but the mobilities of holes are higher, and, as a consequence, $LaNi_{0.6}Fe_{0.4}O_{3-\delta}$ is a p-type conductor.

Acknowledgments

This work was supported by the Centres of Excellence Program at Ural Federal University, Russia.

References

1 M. Zinkevich and F. Aldinger, *Journal of Alloys and Compounds*, 2004, **375**, 147 – 161.

2 R. Chiba, F. Yoshimura and Y. Sakurai, *Solid State Ionics*, 1999, **124**, 281 – 288.

3 K. Kammer, L. Mikkelsen and J. B. Bilde-Srensen, *Journal of Solid State Electrochemistry*, 2006, **10**, 934–940.

4 S. Sugita, Y. Yoshida, H. Orui, K. Nozawa, M. Arakawa and H. Arai, *Journal of Power Sources*, 2008, **185**, 932 – 936.

5 J. Chen, S. Wang, T. Wen and J. Li, *Journal of Alloys and Compounds*, 2009, **487**, 377 – 381.

6 J. Hou, Z. Zhu, J. Qian and W. Liu, *Journal of Power Sources*, 2014, **264**, 67 – 75.

7 Z. Zhu, J. Qian, Z. Wang, J. Dang and W. Liu, *Journal of Alloys and Compounds*, 2013, **581**, 832 – 835.

8 L. Millar, H. Taherparvar, N. Filkin, P. Slater and J. Yeomans, *Solid State Ionics*, 2008, **179**, 732 – 739.

9 A. Morán-Ruiz, K. Vidal, M. Á. Laguna-Bercero, A. Larrañaga and M. I. Arriortua, *Journal of Power Sources*, 2014, **248**, 1067 – 1076.

10 H. Arandiyan, J. Li, L. Ma, S. M. Hashemnejad, M. Z. Mirzaei, J. Chen, H. Chang, C. Liu, C. Wang and L. Chen, *Journal of Industrial and Engineering Chemistry*, 2012, **18**, 2103 – 2114.

11 A. Jahangiri, H. Aghabozorg and H. Pahlavanzadeh, *International Journal of Hydrogen Energy*, 2013, **38**, 10407 – 10416.

12 J. Y. Chen, J. Rebello, V. Vashook, D. M. Trots, S. R. Wang, T. L. Wen, J. Zosel and U. Guth, *Solid State Ionics*, 2011, **192**, 424 – 430.

13 E. Niwa, C. Uematsu, J. Mizusaki and T. Hashimoto, *ECS Transactions*, 2013, **57**, 2133 – 2140.

14 R. N. Basu, F. Tietz, E. Wessel, H. P. Buchkremer and D. Stver, *Materials Research Bulletin*, 2004, **39**, 1335 – 1345.

15 T. Ohzeki, T. Hashimoto, K. Shozugawa and M. Matsuo, *Solid State Ionics*, 2010, **181**, 1771 – 1782.

16 X.-D. Zhou, J. B. Yang, E.-C. Thomsen, Q. Cai, B. J. Scarfino, Z. Nie, G. W. Coffey, W. J. James, W. B. Yelon, H. U. Anderson and L. R. Pederson, *Journal of The Electrochemical Society*, 2006, **153**, J133–J138.

17 E. A. Kiselev and V. A. Cherepanov, *Solid State Ionics*, 2011, **191**, 32 – 39.

18 E. A. Kiselev and V. A. Cherepanov, *Journal of Solid State Chemistry*, 2010, **183**, 1992 – 1997.

19 K. Iwasaki, T. Ito, M. Yoshino, T. Matsui, T. Nagasaki and Y. Arita, *Journal of Alloys and Compounds*, 2007, **430**, 297 – 301.

20 D. S. Tsvetkov, V. V. Sereda and A. Yu. Zuev, *Solid State Ionics*, 2010, **180**, 1620 – 1625.

21 A. Yu. Zuev, A. I. Vylkov, A. N. Petrov and D. S. Tsvetkov, *Solid State Ionics*, 2008, **179**, 1876 – 1879.

22 S. R. Sehlin, H. U. Anderson and D. M. Sparlin, *Phys. Rev. B*, 1995, **52**, 11681 – 11689.

23 A. Aguadero, L. Fawcett, S. Taub, R. Woolley, K.-T. Wu, N. Xu, J. Kilner and S. Skinner, *Journal of Materials Science*, 2012, **47**, 3925–3948.

24 A. Jones and M. S. Islam, *The Journal of Physical Chemistry C*, 2008, **112**, 4455–4462.

25 M. Takano, N. Nakanishi, Y. Takeda, S. Naka and T. Takada, *Materials Research Bulletin*, 1977, **12**, 923 – 928.

26 Y. Takeda, S. Naka, M. Takano, T. Shinjo, T. Takada and M. Shimada, *Materials Research Bulletin*, 1978, **13**, 61 – 66.

27 P. Battle, T. Gibb and S. Nixon, *Journal of Solid State Chemistry*, 1988, **77**, 124 – 131.

28 M. Gateshki, L. Suescun, S. Kolesnik, J. Mais, K. Świerczek, S. Short and B. Dabrowski, *Journal of Solid State Chemistry*, 2008, **181**, 1833 – 1839.

29 M. Idrees, M. Nadeem, M. Shah and T. J. Shin, *Journal of Physics D: Applied Physics*, 2011, **44**, 455303.

30 T. Hashimoto, E. Niwa, C. Uematsu, E. Miyashita, T. Ohzeki, K. Shozugawa and M. Matsuo, *Hyperfine Interactions*, 2012, **206**, 47–50.

31 A. Yu. Zuev and D. S. Tsvetkov, *Solid State Ionics*, 2010, **181**, 557 – 563.

32 A. Yu. Zuev, V. V. Sereda and D. S. Tsvetkov, *Journal of The Electrochemical Society*, 2012, **159**, F594–F599.

33 A. Yu. Zuev and D. S. Tsvetkov, in *Perovskite: Crystallography, Chemistry and Catalytic Performance*, ed. J. Zhang and H. Li, Nova Science Publishers, 2013, ch. Defect Structure and Defect-induced Expansion of Perovskite Oxides.

34 A. Yu. Zuev, V. V. Sereda and D. S. Tsvetkov, *Journal of The Electrochemical Society*, 2014, **161**, F3032–F3038.

35 A. Zuev, V. Sereda and D. Tsvetkov, *International Journal of Hydrogen Energy*, 2014, **39**, 21553 – 21560.

36 R. D. Shannon, *Acta Crystallographica Section A*, 1976, **32**, 751–767.

37 D. Baskar and S. B. Adler, *Chemistry of Materials*, 2008, **20**, 2624–2628.

38 A. Feldhoff, J. Martynczuk, M. Arnold, M. Myndyk, I. Bergmann, V. Šepelák, W. Gruner, U. Vogt, A. Hähnel and J. Woltersdorf, *Journal of Solid State Chemistry*, 2009, **182**, 2961 – 2971.

39 A. B. Makhdoomi, M. Ikram and R. Kumar, *Journal of Magnetism and Magnetic Materials*, 2010, **322**, 2581 – 2584.

40 M. Idrees, M. Nadeem and M. Siddique, *Current Applied Physics*, 2013, **13**, 448 – 452.

41 S. R. Bishop, D. Marrocchelli, C. Chatzichristodoulou, N. H. Perry, M. B. Mogensen, H. L. Tuller and E. D. Wachsman, *Annual Review of Materials Research*, 2014, **44**, 6.1–6.35.

42 M. Nishi, T. Horita, K. Yamaji, H. Yokokawa, T. Shimonosono, H. Kishimoto, M. E. Brito, D. H. Cho and F. Wang, *ECS Transactions*, 2012, **45**, 171 – 180.

43 V. A. Cherepanov, A. N. Petrov and A. Yu. Zuev, in *Solid State Electrochemistry I*, ed. V. Kharton, Wiley-VCH, Weinheim, 2009, ch. Defect Equilibria in Solids and Related Properties: An Introduction.

44 R. R. Heikes and R. W. Ure, *Thermoelectricity: Science and Engineering*, N.Y. : Interscience Pubs, 1961.

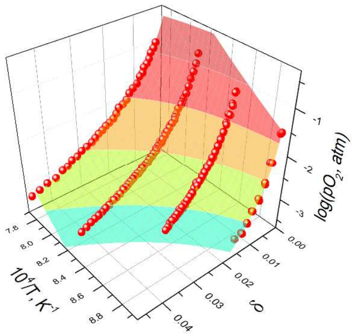

This paper presents original results on oxygen nonstoichiometry and defect structure modeling of $LaNi_{0.6}Fe_{0.4}O_{3-\delta}$ in relation to its physico-chemical properties.

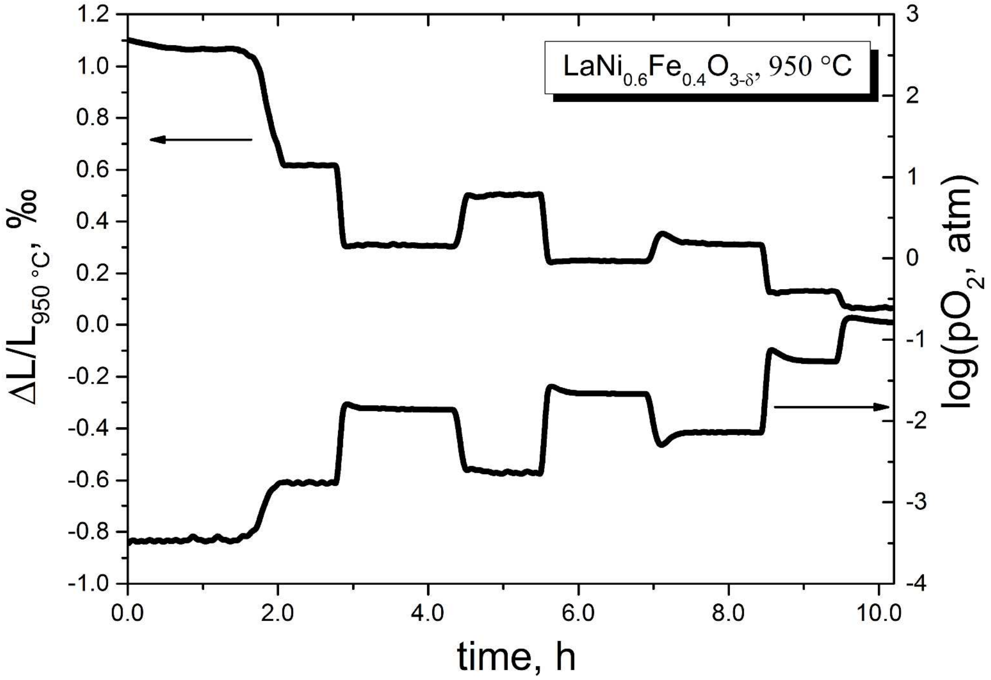
LaNi$_{0.6}$Fe$_{0.4}$O$_{3-\delta}$, 950 °C
ΔL/L$_{950\ °C}$, ‰
log(pO$_2$, atm)
time, h
1.2
1.0
0.8
0.6
0.4
0.2
0.0
-0.2
-0.4
-0.6
-0.8
-1.0
3
2
1
0
-1
-2
-3
-4
0.0
2.0
4.0
6.0
8.0
10.0

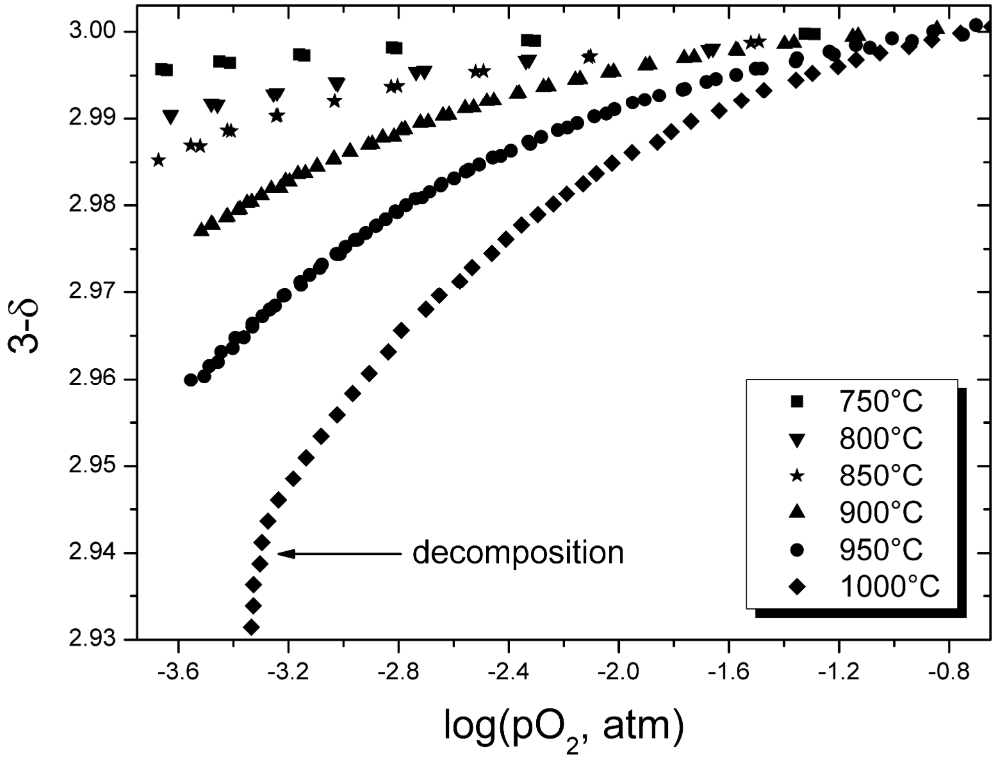
3.00
2.99
2.98
2.97
2.96
2.95
2.94
2.93
3-δ
-3.6
-3.2
-2.8
-2.4
-2.0
-1.6
-1.2
-0.8
log(pO$_2$, atm)
decomposition
■ 750°C
▼ 800°C
★ 850°C
▲ 900°C
● 950°C
◆ 1000°C

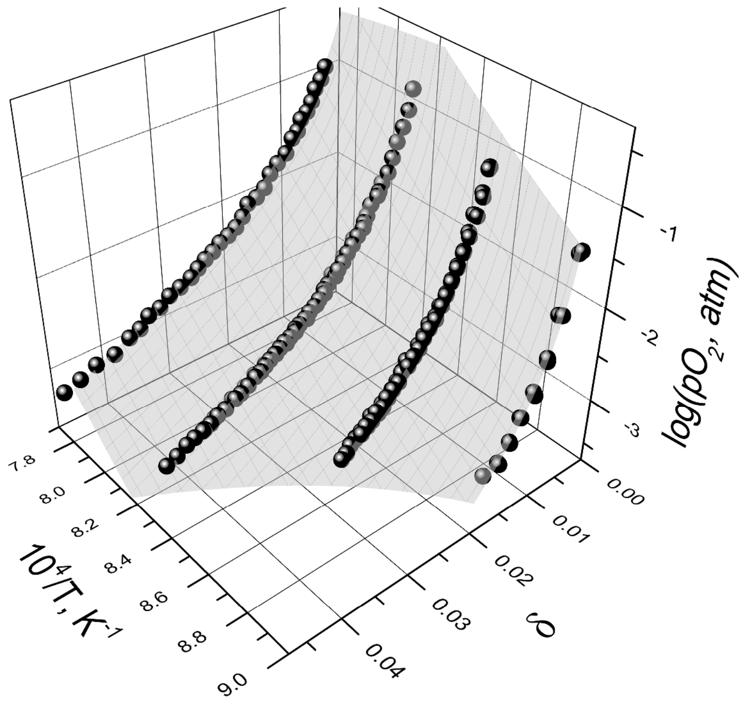
log(pO$_2$, atm)
-1
-2
-3
0.00
0.01
0.02
0.03
0.04
δ
7.8
8.0
8.2
8.4
8.6
8.8
9.0
10^4/T, K^{-1}

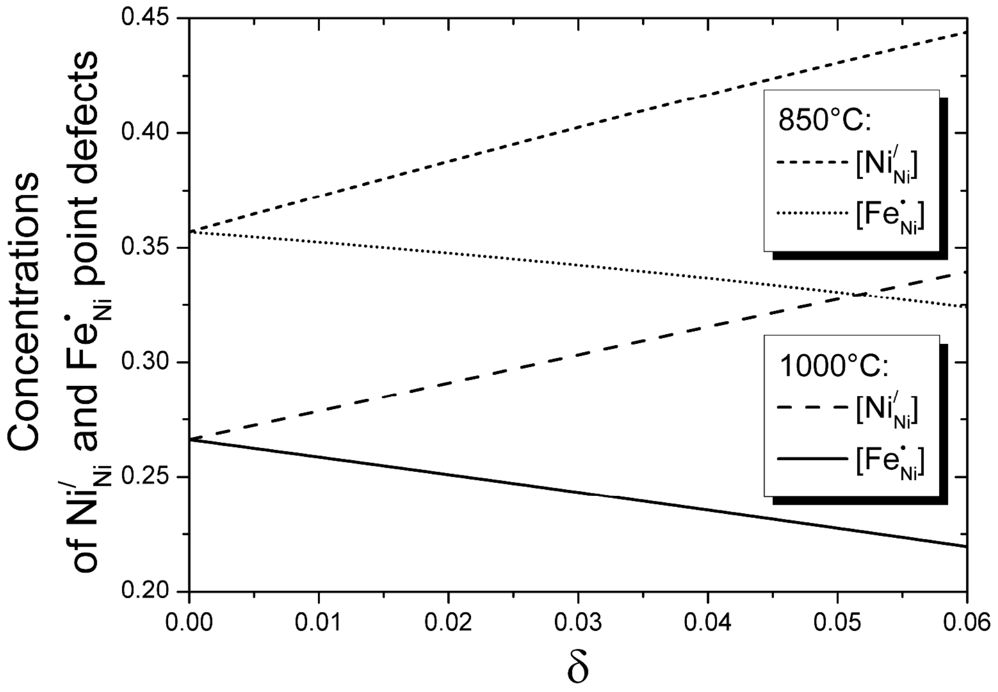
Concentrations
of $Ni_{Ni}^{/}$ and $Fe_{Ni}^{\bullet}$ point defects
0.45
0.40
0.35
0.30
0.25
0.20
0.00
0.01
0.02
0.03
0.04
0.05
0.06
δ
850°C:
$[Ni_{Ni}^{/}]$
$[Fe_{Ni}^{\bullet}]$
1000°C:
$[Ni_{Ni}^{/}]$
$[Fe_{Ni}^{\bullet}]$

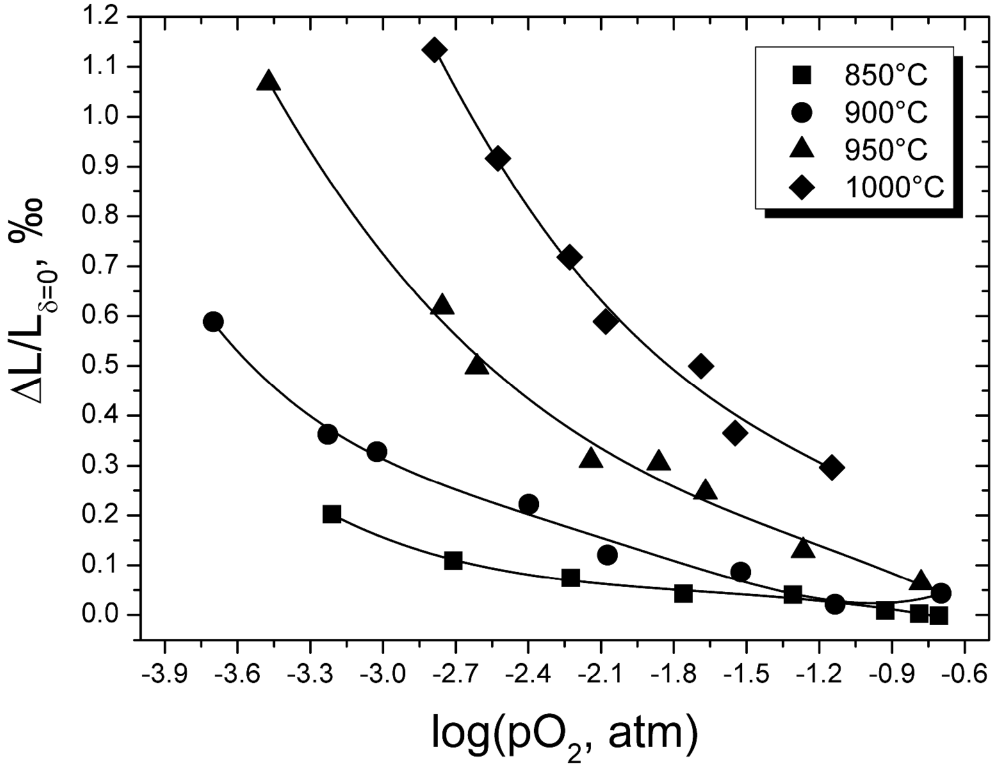

1.2
1.1
1.0
0.9
0.8
0.7
0.6
0.5
0.4
0.3
0.2
0.1
0.0
$\Delta L/L_{\delta=0}$, ‰
■ 850°C
● 900°C
▲ 950°C
◆ 1000°C
-3.9
-3.6
-3.3
-3.0
-2.7
-2.4
-2.1
-1.8
-1.5
-1.2
-0.9
-0.6
log(pO_2, atm)

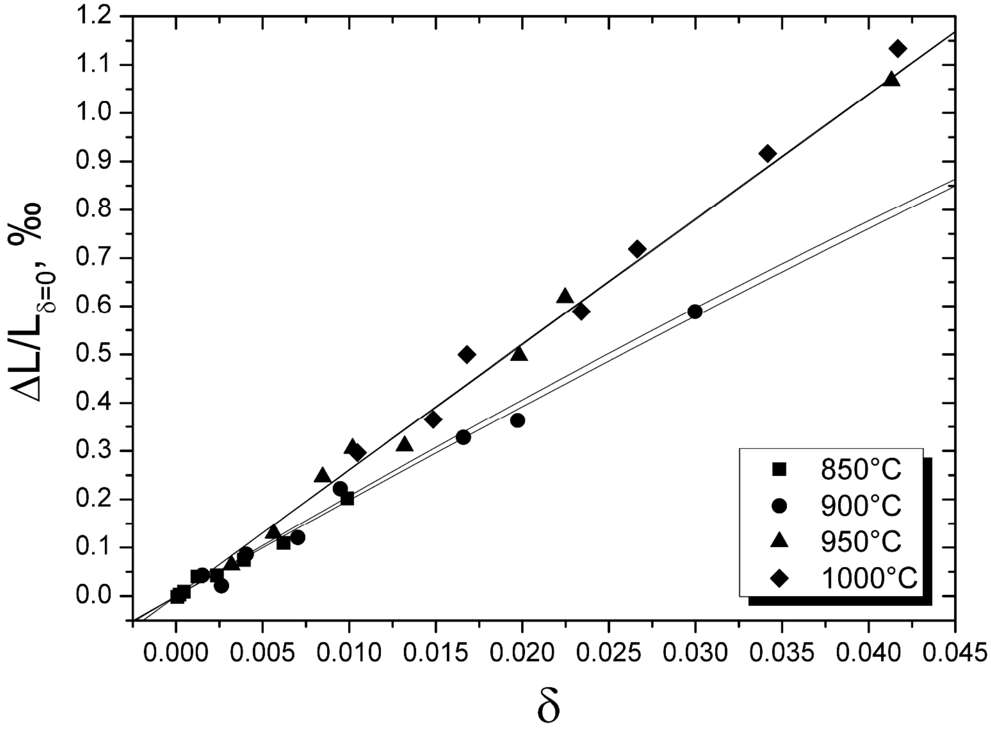

1.2
1.1
1.0
0.9
0.8
0.7
0.6
0.5
0.4
0.3
0.2
0.1
0.0
$\Delta L/L_{\delta=0}$, ‰
0.000
0.005
0.010
0.015
0.020
0.025
0.030
0.035
0.040
0.045
δ
■ 850°C
● 900°C
▲ 950°C
◆ 1000°C

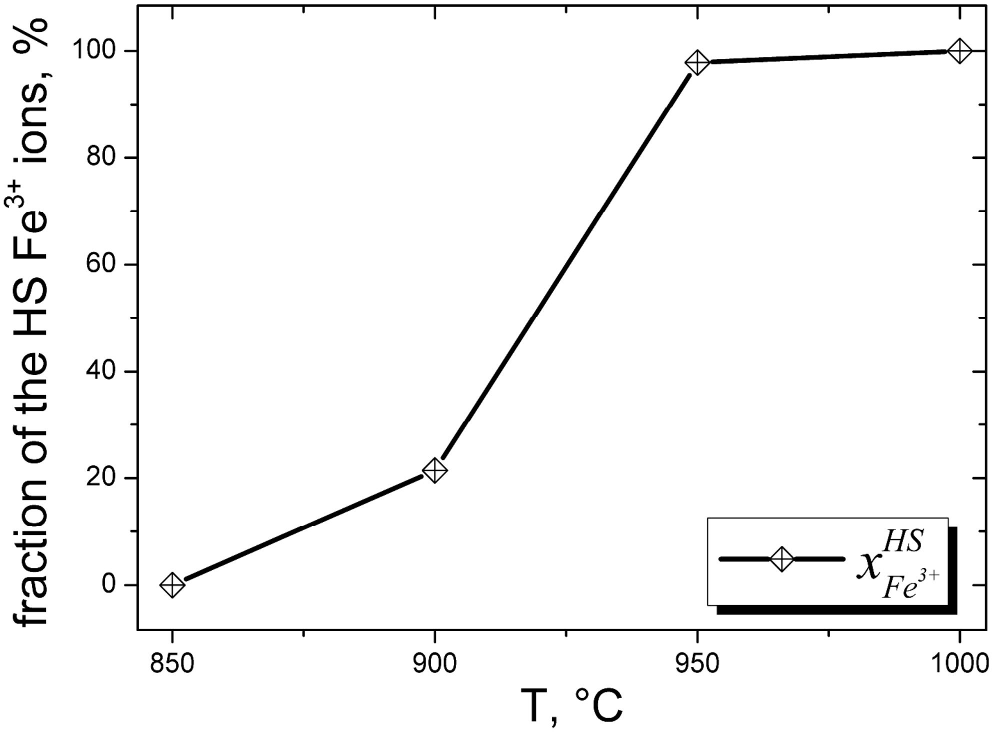
fraction of the HS Fe^{3+} ions, %
100
80
60
40
20
0
850
900
950
1000
T, °C
$x^{HS}_{Fe^{3+}}$

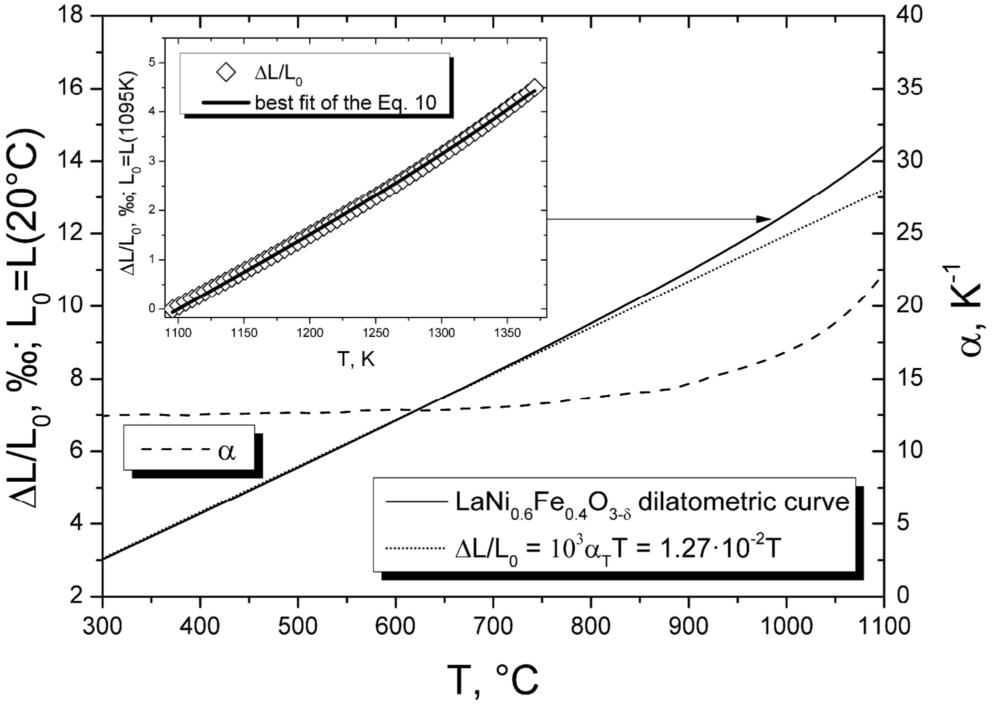
ΔL/L₀, ‰; L₀=L(20°C)
α, K⁻¹
T, °C
300
400
500
600
700
800
900
1000
1100
2
4
6
8
10
12
14
16
18
0
5
10
15
20
25
30
35
40
α
LaNi0.6Fe0.4O3-δ dilatometric curve
ΔL/L₀ = 10³αTT = 1.27·10⁻²T
ΔL/L₀
best fit of the Eq. 10
ΔL/L₀, ‰; L₀=L(1095K)
T, K
1100
1150
1200
1250
1300
1350
0
1
2
3
4
5

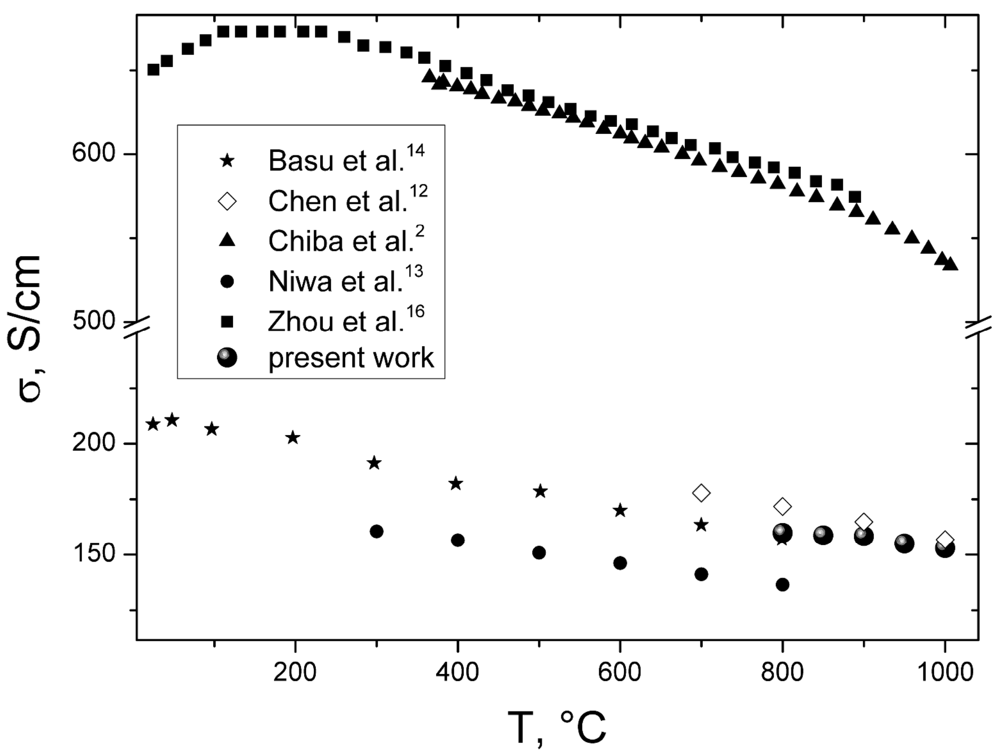
σ, S/cm
T, °C
600
500
200
150
200
400
600
800
1000
★ Basu et al.[14]
◇ Chen et al.[12]
▲ Chiba et al.[2]
● Niwa et al.[13]
■ Zhou et al.[16]
● present work

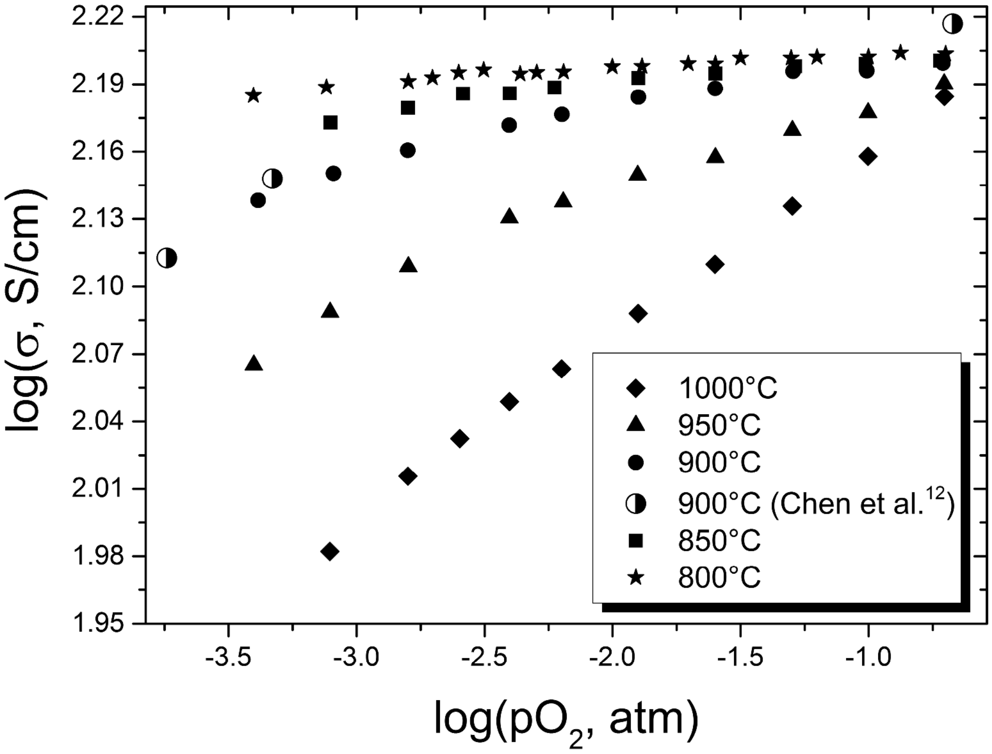
log(σ, S/cm)
log(pO₂, atm)
2.22
2.19
2.16
2.13
2.10
2.07
2.04
2.01
1.98
1.95
-3.5
-3.0
-2.5
-2.0
-1.5
-1.0
◆ 1000°C
▲ 950°C
● 900°C
◑ 900°C (Chen et al.12)
■ 850°C
★ 800°C

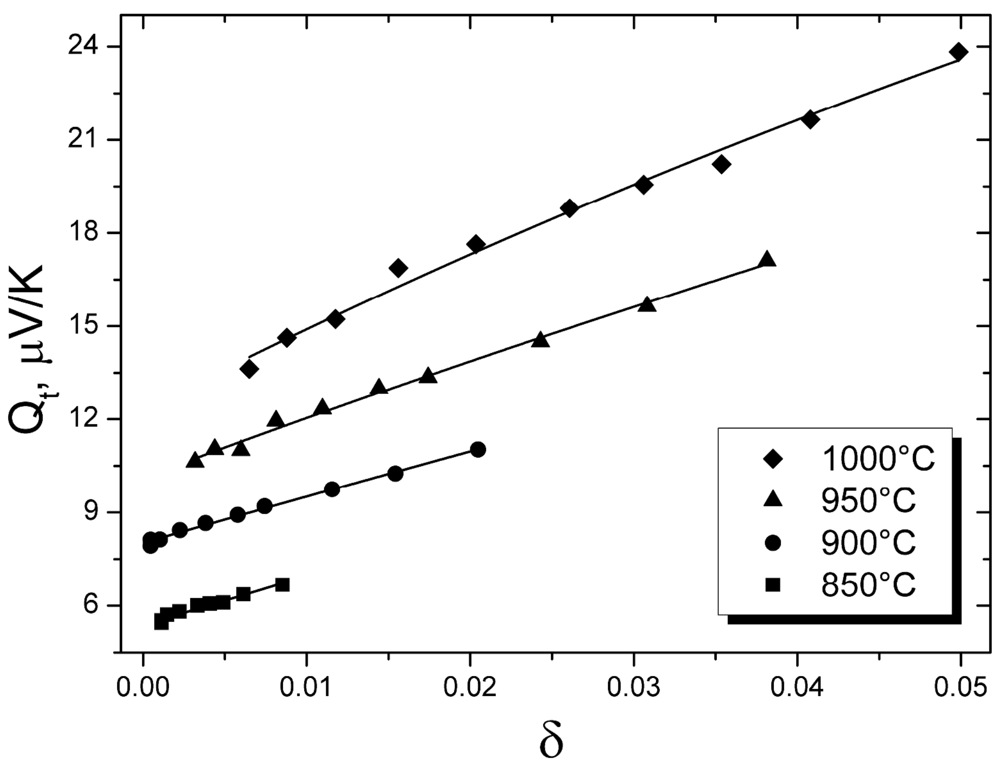

24
21
18
15
12
9
6
0.00
0.01
0.02
0.03
0.04
0.05
Q_t, μV/K
δ
◆ 1000°C
▲ 950°C
● 900°C
■ 850°C

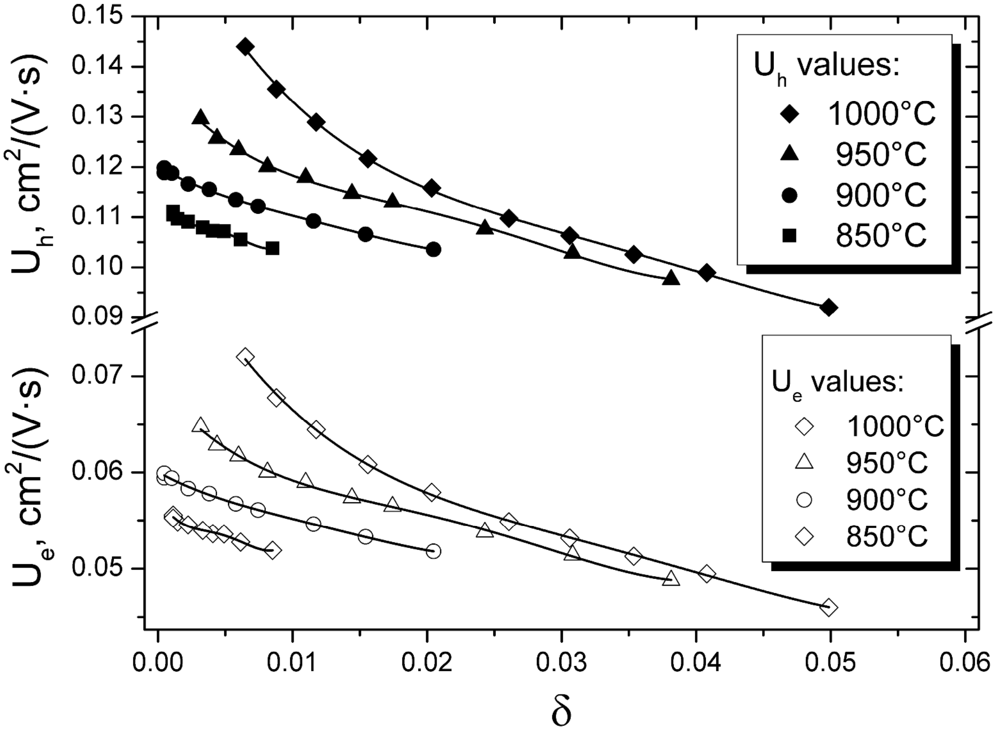

U_h, cm^2/(V·s)
U_e, cm^2/(V·s)
δ
0.15
0.14
0.13
0.12
0.11
0.10
0.09
0.07
0.06
0.05
0.00
0.01
0.02
0.03
0.04
0.05
0.06
U_h values:
◆ 1000°C
▲ 950°C
● 900°C
■ 850°C
U_e values:
◇ 1000°C
△ 950°C
○ 900°C
◇ 850°C